Chapter 7 Systematic Methodology of Earth-Moon Transfer Trajectory Design with Gravitational Capture

This chapter focuses on trajectory design method for earth-moon transfer which fully takes advantage of gravitational capture mechanism. In the course of orbit design, we assume that two analyses concerning gravitational capture (Chapter 4) and solar effect (Chapter 6) are given beforehand which provide the outline of orbital profile to considerable extent. A systematic orbit design method, with previously given information, is newly proposed and applied for earth-moon path construction in multi-body system.

7.1 Formulation of Earth-Moon Transfer Trajectory Design

From the numerical analysis of gravitational capture (Chapter 4), semi-major axis and perigee distance conditions prior to gravitational capture was obtained. Besides, orbital shape in the vicinity of the moon as well as resultant perilune conditions at lunar insertion point were given. On the whole, Chapter 4 describes the orbital profile of near-capture phase of earth-moon transfer trajectory. On the other hand, the analysis of solar effect in sun-earth-S/C three-body system (Chapter 6) provides possible orbital profile of geocentric portion of earth-moon transfer which satisfies pre-capture conditions given in Chapter 4.

With the accumulated information through these two analyses, potential way for effective procedure for earth-moon transfer trajectory design is discussed in this section.

7.1.1 Miscellaneous Approaches for Earth-Moon Path Construction with Gravitational Capture

We can imagine as an ideal case that earth-moon transfer trajectory is accomplished without using correction maneuver en route to the goal, namely lunar insertion point. Actually, it is possible to construct this 'natural' type transfer in a troublesome way. For example, firstly, assume a perilune at a certain location corresponding to the mission

objective. Secondly, propagate in backward time from perilune and see whether S/C could reach the earth within a reasonable flight time. If not, search perilune velocity until trajectory reaches the earth with prespecified perigee distance. By this trial and error method, so to say, we can for the time being obtain what we call 'natural' earth-moon transfer trajectory with gravitational capture at moon. However, sensitivity to perilune velocity is so high that it is nearly impossible to adopt this method from practical point of view. Besides, this method is not able to utilize the previously given information.

Here, midcourse velocity correction is introduced taking advantage of artificial spacecraft controllability. First, single delta-V case is considered. Single midcourse maneuver requires direct targeting from both earth departure and lunar insertion point (see Fig.7-1). However, this approach is still extremely sensitive for targeting due to high nonlinearity. Similar concept was utilized by J.Miller et al.[67].

Next, to relieve this high nonlinearity, velocity correction opportunity is doubled (see Fig.7-2). Namely, in the first place, trajectories starting from perigee and perilune are propagated in forward and backward time for a certain flight time respectively. Secondly, these terminal trajectories are connected by some targeting method. This achieves earth-moon transfer for the time being which includes velocity correction twice at terminal points for targeting.

Still there is quite a problem to solve. Amount of midcourse maneuvers is generally beyond the capability of spacecraft and hard to reduce, since it is quite sensitive to boundary conditions at earth departure as well as lunar insertion. Thereby, for refining the boundary conditions, some optimization method is needed.

7.1.2 Formulation as a Parameter Optimization Problem

Now, attention is paid to well-known design approach of multi-swingby orbit. It is conventionally constructed as parameter optimization problem, where control parameters are constituted of B-plane parameters (see Appendix J). The sum of trajectory correction maneuver is usually taken as performance index. For the generation of trajectory, patched

conic method [87-88] as well as multi-conic method [89-90] are occasionally utilized (see Appendix F for multi-conic method).

Here, this concept is extended to gravitational capture orbit. In gravitational capture orbit, two-body conic approximation is insufficient from precision point of view even for preliminary analysis, as can be imagined from the studies in previous chapters. This inevitably requires trajectory generation in multi-body system consisting of at least three bodies.

With this observation, we construct a novel trajectory construction procedure for earth-moon transfer with gravitational capture, whose underlying concept is parameter optimization. Characteristics of the proposed method are as follows (see Fig.7-3);

(a) Earth-moon transfer trajectory is divided into three segments, by which inherent sensitivity to boundary conditions at earth departure and lunar insertion is localized and lowered as well. The length of each segment is arbitrarily selected.
(b) Results of analyses concerning gravitational capture (Chapter 4) as well as solar effect (Chapter 6) are effectively utilized for the initial guess of control parameters, i.e. boundary conditions.
(c) Midcourse velocity correction is taken into account by use of FTA target which connects two terminal trajectory segments (inner loop) (cf. Appendix G for FTA target).
(d) Control parameters are updated and optimized so that performance index constituted of total velocity correction maneuver is minimized (outer loop).

It may be said the use of midcourse maneuvers alleviates the high nonlinearity inherent to gravitational capture mechanism, and simultaneously enhances feasibility of orbital profile. Precise scheme of the proposed orbit design method is shown below.

(1) Control Parameters

As to control parameters, the following are possibly utilized which correspond to boundary conditions at earth departure and lunar insertion (see Fig.7-4). Control parameters shown here are for planar case (i.e.within the plane defined by earth-moon motion), while perigee and perilune distances are assumed to be given;

a) perigee velocity and position at earth departure ($V_{perigee}$, $\theta_{perigee}$),

b) perilune velocity and position at lunar insertion ($V_{perilune}$, $\theta_{perilune}$),

c) total flight time (t_{total}),

d) sun phase defined at a certain epoch (α),

e.g. moon's position in sun-earth fixed rotating frame at lunar orbit insertion,

e) epochs at both ends of intermediate trajectory segment (t_1, t_2),

Initial guess of parameters b) is obtained from the analysis of gravitational capture, while parameters a), c) and d) are from that of solar effect. Here, we handle them as control parameter vector X as follows;

$$X^T = (V_{perigee}, \theta_{perigee}, V_{perilune}, \theta_{perilune}, t_{total}, \alpha, t_1, t_2) \qquad (7\text{-}1)$$

Control parameters are arbitrary in number and flexibly chosen corresponding to the mission objective. For example, when out-of-plane motion has to be taken into account, it can be responded by introducing control parameters such as inclination and ascending node.

(2) Fixed Time-of-Arrival Target (Inner Loop)

For the inner loop, first, two trajectory segments, earth-departure and lunar capture legs, are propagated forward and backward respectively, assuming some boundary conditions given by control parameter X. Then FTA target is utilized for connecting these two terminal trajectory segments (see Fig.7-3). This inner loop procedure assures earth-

moon transfer closed path for the time being, setting aside the amount of midcourse maneuvers.

(3) Performance Index

Performance index consists of cost function and penalty function. Cost function is defined as the sum of trajectory correction maneuvers at both ends of intermediate trajectory segment for FTA target. The reduction of this cost function would realize earth-moon transfer with reasonable delta-V.

Penalty function may be introduced as additive term to cost function. Apogee position information or swingby distance constraint may be included in this penalty function corresponding to the orbital profile. They are summarized as follows;

Cost function	The sum of trajectory correction maneuvers at terminal points of FTA target	$\Delta V_1+\Delta V_2$
Penalty function	Apogee position information	Δr_{apo}, $\Delta\theta_{apo}$
	Swingby distance constraint	Δr_{swb}

Performance index

Performance index consists of cost and penalty function as shown below.

$$F = f_1\Delta V_1{}^T\Delta V_1 + f_2\Delta V_2{}^T\Delta V_2 + f_3\Delta r_{apo}{}^2 + f_4\Delta\theta_{apo}{}^2 + f_5\Delta r_{swb}{}^2 \qquad (7\text{–}2)$$

where f_1, f_2, f_3, f_4, f_5 are weight factors as follows (f_3, f_4, f_5 may take null value);

$$f_1 = \frac{1}{|\Delta V_1|}, \; f_2 = \frac{1}{|\Delta V_2|}, \text{ etc.} \qquad (7\text{-}3)$$

(4) Modified Newton Algorithm (Outer Loop)

Modified Newton algorithm is used for obtaining optimal control parameters by minimizing performance index. Its algorithm is summarized below.

Modified Newton algorithm

Derivative of performance index F with regard to control parameter vector X, g, is expressed as follows;

$$g^T = \frac{\partial F}{\partial X} = 2\, f_1\, \Delta V_1{}^T \frac{\partial \Delta V_1}{\partial X} + 2\, f_2\, \Delta V_2{}^T \frac{\partial \Delta V_2}{\partial X} + 2\, f_3\, \Delta r_{apo} \frac{\partial \Delta r_{apo}}{\partial X} + 2\, f_4\, \Delta \theta_{apo} \frac{\partial \Delta \theta_{apo}}{\partial X} + 2\, f_5\, \Delta r_{swb} \frac{\partial \Delta r_{swb}}{\partial X} \qquad (7\text{–}4)$$

Second derivative of performance index F, H (Hessian), has the following form.

$$\begin{aligned} H = \frac{\partial^2 F}{\partial X^2} = {} & 2f_1 \left(\Delta V_1{}^T \frac{\partial^2 \Delta V_1}{\partial X^2} + \frac{\partial \Delta V_1{}^T}{\partial X} \frac{\partial \Delta V_1}{\partial X} \right) \\ & + 2f_2 \left(\Delta V_2{}^T \frac{\partial^2 \Delta V_2}{\partial X^2} + \frac{\partial \Delta V_2{}^T}{\partial X} \frac{\partial \Delta V_2}{\partial X} \right) \\ & + 2f_3 \left(\Delta r_{apo}{}^T \frac{\partial^2 \Delta r_{apo}}{\partial X^2} + \frac{\partial \Delta r_{apo}{}^T}{\partial X} \frac{\partial \Delta r_{apo}}{\partial X} \right) \\ & + 2f_4 \left(\Delta \theta_{apo}{}^T \frac{\partial^2 \Delta \theta_{apo}}{\partial X^2} + \frac{\partial \Delta \theta_{apo}{}^T}{\partial X} \frac{\partial \Delta \theta_{apo}}{\partial X} \right) \\ & + 2f_5 \left(\Delta r_{swb}{}^T \frac{\partial^2 \Delta r_{swb}}{\partial X^2} + \frac{\partial \Delta r_{swb}{}^T}{\partial X} \frac{\partial \Delta r_{swb}}{\partial X} \right) \end{aligned} \qquad (7\text{–}5)$$

which is approximated as follows postulating that second derivative of each term constituting performance index can be ignored when compared with its first derivative;

$$\begin{aligned} H = \frac{\partial^2 F}{\partial X^2} = {} & 2f_1 \left(\frac{\partial \Delta V_1{}^T}{\partial X} \frac{\partial \Delta V_1}{\partial X} \right) + 2f_2 \left(\frac{\partial \Delta V_2{}^T}{\partial X} \frac{\partial \Delta V_2}{\partial X} \right) \\ & + 2f_3 \left(\frac{\partial \Delta r_{apo}{}^T}{\partial X} \frac{\partial \Delta r_{apo}}{\partial X} \right) + 2f_4 \left(\frac{\partial \Delta \theta_{apo}{}^T}{\partial X} \frac{\partial \Delta \theta_{apo}}{\partial X} \right) + 2f_5 \left(\frac{\partial \Delta r_{swb}{}^T}{\partial X} \frac{\partial \Delta r_{swb}}{\partial X} \right) \end{aligned} \qquad (7\text{–}6)$$

Now, performance index F and its derivative g are expanded in Taylor series around X_0 as shown below,

$$F = F_0 + g_0^T(X-X_0) + \frac{1}{2}(X-X_0)^T H_0(X-X_0) + \ldots \quad (7\text{–}7)$$

$$g = g_0 + H_0(X-X_0) \ldots . \quad (7\text{–}8)$$

Provided there exists local minimum of performance index, control parameter vector X is updated to minimize performance index F in the following manner

$$X = X_0 - \gamma H_0^{-1} g \quad (7\text{–}9)$$

where optimal coefficient γ is determined by linear search in the optimal direction expressed by $H_0^{-1}g$. Eq.(7-9) is obtained by equating the right side of Eq.(7-8) to zero. When the difference in performance index, between the states before and after updating control parameters, gets lower than a certain value, it is regarded as converged.

(5) Apogee Information

The proposed method is able to make use of apogee information derived in the analysis of solar effect in sun-earth-S/C three-body system (see Chapter 6). Apogee positional phase and its geocentric distance may be included in penalty function as additive term of performance index (see Sec.7.1.2.(3)). At the initial stage of convergence, this works as an insurance against trajectory divergence from what was originally aimed at.

(6) Use of Lunar Swingby

When lunar swingby is utilized after earth departure, orbit design would be considerably complicated since phasing of the moon between lunar swingby and lunar orbit insertion have to be taken into consideration.

In the proposed method, use of lunar swingby is coped with as follows; initial guess of total flight time is calculated so that both apogee position and lunar swingby lie in the same direction in sun-earth fixed rotating frame as seen from the earth (see Fig.7-5). As though in the use of apogee information, lunar swingby distance may be included in penalty function to ensure lunar swingby use.

7.2 Orbit Design in Multi-Body System

In this section, earth-moon transfer trajectory with gravitational capture is actually designed in multi-body system using the proposed method. Various profile orbits are designed with the variation on the revolution number around the earth, on the use of lunar swingby and on capture direction at perilune.

Sun-earth-moon-S/C four-body system is assumed for the model, where sun, earth and moon move in the same plane (see Appendix D). However, the discussion hereafter may well adopt precise model with planetary ephemeris, since model error such as solar pressure and inclination of moon's motion w.r.t. the ecliptic plane is negligible, and hardly affects the orbit design procedure based on the previous analyses in simplified model (i.e. earth-moon-S/C three-body model in Chapter 4 and sun-earth-S/C three-body model in Chapter 6).

Fig.7-6 through Fig.7-15 show several examples of earth-moon transfer trajectory with gravitational capture at moon. They are numbered from orbit 1 to orbit 10. Each orbital profile is plotted in geocentric sun-earth fixed frame as well as in inertial frame. Moreover, earth-moon fixed frame is used to describe trajectories in the vicinity of the moon. Their orbital sequences with numerical data are tabulated in Table 7-1.

Perigee altitude at earth departure is assumed at 200km, while perilune height at lunar orbit insertion is frozen at 100km. Lunar insertion points are located at earth side on or near earth-moon line except for orbit 9, where perilune is situated over lunar north pole. Perilunes are attained by in-plane direct capture for orbit 1~6, 8 and 10. Orbit 7 and 9 realize in-plane retrograde capture and polar capture, severally.

Concerning orbital profile, orbit 1~4 and orbit 7~9 depict single revolution around the earth, while orbit 5 and 6 accompany double revolutions. Orbit 8 realizes so-called 'natural capture' since S/C rotates around the moon after approaching from outside the moon's sphere of influence, essentially without trajectory correction maneuver. Orbit 10 embodies Halo-type earth-moon transfer where exist three apogees as local maxima of geocentric distance.

S/C incorporates lunar swingby right after earth departure in orbit 3 through orbit 10. And in every case (orbit 1~10), final approach to the moon is from anti-earth side as discussed in Sec.5.3. These observations are clearly derived when seen in earth-moon fixed frame plots.

As to control parameters assumed in orbit design procedure, the following five are used for orbit 1~8 and orbit 10: perigee position and velocity at earth departure, perilune velocity at lunar orbit insertion, total flight time, and sun phase. Exceptionally, polar capture case (orbit 9) requires inclination at earth departure to be the sixth control parameter.

Initial values of control parameters in orbit 2, 4 and 6 correspond to the converged ones of orbit 1, 3 and 5, respectively (see Table 7-2 for numerical data). Concerning penalty function, apogee information is taken into account in orbit 1, 3 and 5, while swingby distance is constrained in orbit 3, 5, 7 and 9 (see Table 7-3, Sec.7.1.2.(5), (6)). Thus, it may be said that orbit 2, 4 and 6, which are exempt from constraints during optimization procedure, are finally obtained from orbit 1, 3 and 5 respectively by further optimization.

Each orbit converged in around 5 loops (15 minutes CPU time in M780 of Fujitsu Ltd.), where one loop corresponds to an update of control parameters (i.e. outer loop). Convergence of trajectories are depicted in Fig.7-16 for orbit 3~6 in sun-earth fixed frame. In Fig.7-17 are illustrated the convergence of performance index and its derivative with respect to control parameters also for orbit 3~6. During design procedure, it was observed

that total trajectory correction maneuver is particularly sensitive to perilune velocity as well as sun phase (not shown in Fig.7-17).

The proposed method shows satisfactory convergence corresponding to initially guessed control parameters through the information of Chapter 4 and 6. Inversely speaking, the analyses concerning gravitational capture (Chapter 4) and solar effect on geocentric orbit (Chapter 6) provide enough information for the design of this kind of trajectory.

7.3 Conventional Approaches for Earth-Moon Transfer

Before proceeding to the discussion of the merit in the use of gravitational capture, conventional approaches for earth-moon transfer are thoroughly investigated. Well-known transfer geometries are Hohmann transfer and bi-elliptic transfer (see Fig.7-18). Bi-parabolic transfer is categorized into an extreme case of bi-elliptic transfer.

Hohmann transfer is optimal in case of transfer from circular (radius r_1) to circular (radius r_2) trajectory by use of two delta-Vs at terminal points. When the ratio r_2/r_1 is larger than 15.58172, bi-elliptic transfer is superior to Hohmann transfer in terms of total delta-V as far as apogee distance is larger than r_2 [91]. When applied to earth-moon transfer, r_1 and r_2 take the value of 6,578km (200km altitude) and 384,400km severally, which yields r_2/r_1 of 58.44. Therefore, bi-elliptic transfer is preferable on the assumption of circular-to-circular transfer.

However, when lunar orbit insertion is taken into account, the result changes drastically. Table 7-4 summarizes required velocity increments in Hohmann, bi-elliptic and bi-parabolic transfers. Delta-V at lunar insertion is calculated based on one-point patched conic method (see Fig.7-18 and Appendix F) except for numerically integrated Hohmann transfer case. Initial earth orbit is assumed to be 200km-altitude circular orbit, and lunar insertion point is fixed at the altitude of 100km. The following three delta-Vs are tabulated: injection at earth departure, delta-V at apogee and required velocity reduction at lunar insertion point into osculating parabolic orbit (i.e.zero C3 w.r.t. moon). Fig.7-19 focuses

on bi-elliptic transfer where magnitude of each delta-V is shown as a function of apogee distance.

It is shown in Table 7-4 and also in Fig.7-19 that bi-elliptic transfer becomes equivalent to Hohmann transfer in terms of total delta-V, only when its apogee distance is as much as 28,200,000km (comparison is made for one-point patched conic cases). This in turn states that bi-elliptic transfer, to say nothing of bi-parabolic transfer, is quite impractical from flight time point of view when lunar orbit insertion is considered. Based on these results, gravitational capture type earth-moon transfer is mainly compared with Hohmann-type transfer in the following section.

7.4 Comparison in Delta-V and Flight Time

Table 7-5 summarizes previously designed gravitational capture trajectory (orbit 1~10) in terms of flight time and trajectory correction maneuver. Also attached is the optimal Hohmann transfer trajectory information (see Fig.7-20), which is compared with gravitational capture orbits.

Here, Hohmann transfer case is integrated in earth-moon-S/C three-body system, different from gravitational capture orbits. However, it would make negligible difference in total delta-V even if designed in four-body model (i.e. within 1~2 m/s depending on the relative position of the sun), which guarantees the validity of the comparison shown in Table 7-5.

S/C is postulated in a 200km-altitude circular orbit at earth departure, while lunar orbit insertion point is located at the altitude of 100km for every case. Delta-V gain at lunar orbit insertion is defined as the difference between perilune velocity and corresponding osculating parabolic velocity. Every gravitational capture orbit achieves negative value of delta-V gain, since C3 w.r.t. the moon is negative at perilune.

With the use of gravitational capture, flight time of at least three months is needed, while total delta-V is reduced by as much as 150m/s (cf. orbit 4, 7 and 8) in comparison with that of optimal Hohmann-type transfer. If this velocity gain is entirely allotted to the

reaction control system with specific impulse (Isp) of 180sec (300sec), then 9% (5%) of total S/C weight can be saved. These results show that earth-moon transfer trajectory with gravitational capture is practical from delta-V and flight time point of view.

When lunar swingby is utilized after earth departure, around 40m/s is earned at earth injection (compare orbit 1~2 with orbit 3~4). Concerning midcourse delta-Vs, they are almost zero in orbit 2, 4 and 6~8, since orbital configuration was not so constrained in trajectory design procedure (i.e. penalty function was not severe). As to achievable C3 w.r.t. the moon at perilune, polar capture (orbit 9) is inferior to other in-plane captures as discussed in Sec.4-7.

Now, velocity gain produced in gravitational capture type transfer is investigated more precisely. Table 7-6 summarizes what we pursue now. Gravitational capture type trajectory (orbit 4) is compared with Hohmann type as well as with bi-elliptic type transfer with apogee distance of 1,500,000km. The latter resembles gravitational capture type transfer in terms of its orbital shape. Delta-Vs are simply calculated by patched conic method, which provides the ideal case without solar perturbation. As to Hohmann type transfer, it corresponds to optimal case from delta-V point of view and is numerically integrated in earth-moon-S/C three-body model. The validity of using three-body model is noted previously in this section.

It is shown that velocity gain over Hohmann transfer is completely attributed to the low relative velocity with respect to the moon at perilune. On the other hand, velocity gain over bi-elliptic transfer (396m/s in total) is mainly owing to the positive use of solar perturbation whose equivalent delta-V is 281m/s.

7.5 Possible Lunar Insertion Point

As stated in Sec.5.4, one of the merits in using gravitational capture is the wide possible range of lunar insertion points, which has been already pointed out by J.Miller et al.[67]. For in-plane case, possible range is distributed from 0 through 270 deg measured from anti-earth direction for both direct and retrograde capture (see Fig.4-16).

Here, lunar insertion points that can be attained by Hohmann transfer are investigated for comparison. In Hohmann transfer, lunar encounter trajectory is approximated by lunicentric hyperbola which states that argument of perilune is coupled with the direction of approach asymptotes. Therefore, possible range of lunar insertion point is anticipated not so wide.

Fig.7-20 shows total delta-V and flight time with regard to perilune positional phase obtained by numerical integration in earth-moon-S/C three-body system. Fig.7-21 visualizes perilune phases that can be achieved by Hohmann transfer based on Fig.7-20. It is shown that direct capture can attain perilunes located at 170~260deg measured from anti-earth direction, while retrograde capture at -80 through +60deg.

These results validate the merit of gravitational capture in terms of wide range of possible lunar insertion point in comparison with Hohmann transfer. Besides, it is shown that prohibited region for Hohmann transfer (i.e. positional phase of 70~160deg) can be chosen for lunar insertion points if gravitational capture is adopted.

7.6 Launch Window

Finally, launch window analysis is performed based on previously designed trajectories i.e. orbit 2, 4 and 6. Fig.7-22 depicts the relation between launch window (i.e.total flight time) and delta-V gain over Hohmann-type transfer (i.e. optimal case shown in Table 7-5). Corresponding apogee distance and swingby distance are also shown. For each launch date, optimization is performed using the proposed method assuming that lunar insertion point is fixed even launch date is varied.

The width of launch window is estimated around ten days for orbit 2, three days for orbit 4 and only one day for orbit 6. Thus, launch window of gravitational capture type earth-moon transfer considerably depends on its orbital profile.

7.7 Summary (Chapter 7)

A systematic trajectory design procedure for earth-moon transfer trajectory with gravitational capture is newly proposed. Information accumulated through the analyses of gravitational capture (Chapter 4) and solar effect (Chapter 6) is effectively used for initial guess of boundary conditions at earth departure and lunar insertion. Positional continuity required for forming a loop between earth departure and lunar insertion is guaranteed by FTA target method. Then, boundary conditions are optimized by use of modified Newton algorithm.

The proposed method was actually applied to trajectory design in multi-body system with satisfactory convergence. At the same time, it was shown that the analyses of gravitational capture (Chapter 4) and solar effect (Chapter 6) provide sufficient information for the initial guess of the proposed method.

It was also shown that earth-moon transfer trajectory with gravitational capture at moon is practical from flight time and delta-V point of view. Flight time takes the value from three to four months on the average, while the sum of required delta-V can be reduced by approximately 150m/s in comparison with conventional Hohmann-type transfer. This velocity gain is mainly indebted to the low relative velocity (C3) w.r.t. the moon at lunar insertion point, which would save 5% (9%) of S/C mass assuming specific impulse of 300 (180) seconds.

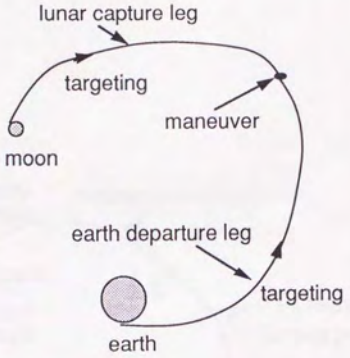

Fig.7-1 Single Velocity Correction Maneuver Approach

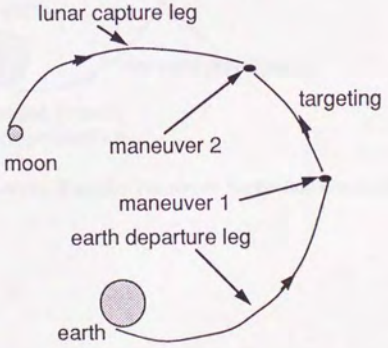

Fig.7-2 Double Velocity Correction Maneuver Approach

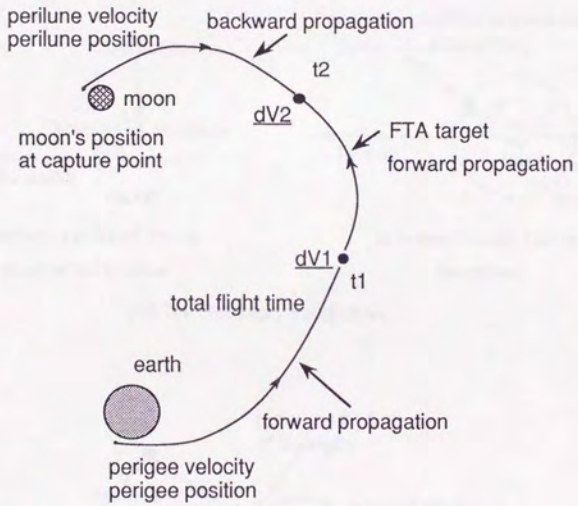

Fig.7-3 Earth-Moon Transfer Trajectory Model and Control Parameters

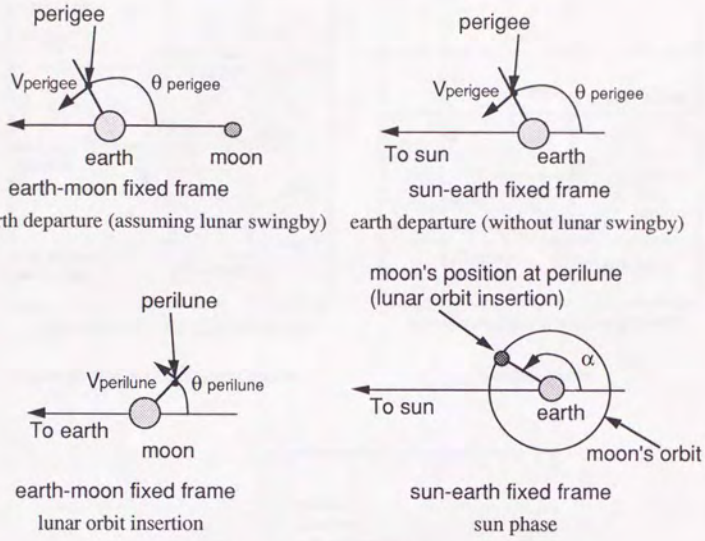

Fig.7-4 Boundary Conditions

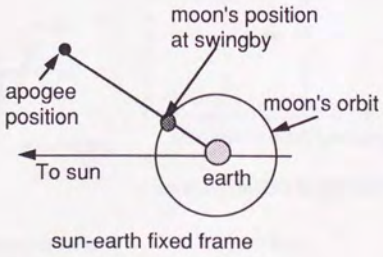

assumption: swingby and apogee position lie on the same direction in sun-earth-fixed frame

Fig.7-5 Initial Guess for Lunar Swingby Geometry

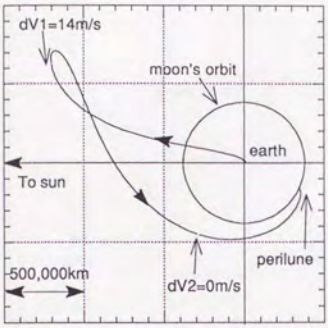

sun-earth-line fixed rotating frame

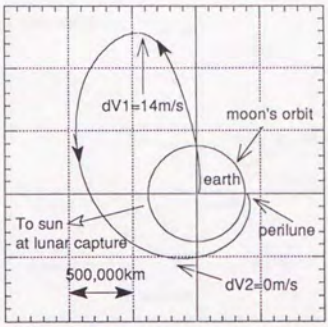

inertial frame

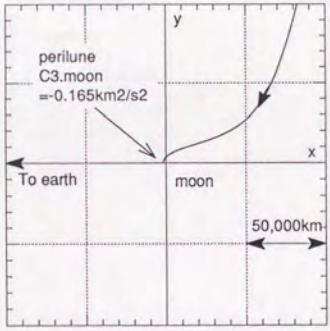

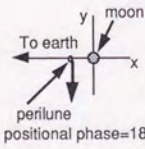

earth-moon-line fixed rotating frame

apogee distance 1,380,193 km
total flight time 102.46 day
dV1 = 14.6 m/s, dV2 = 0.00 m/s
C3 w.r.t. moon at perilune = - 0.165 km^2/s^2 (in-plane direct capture)

Fig.7-6 Orbital Profile (Orbit 1)

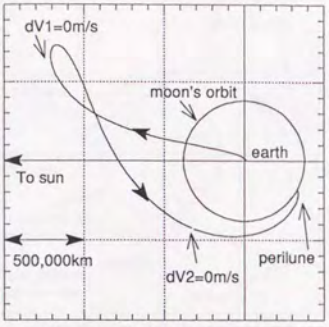

sun-earth-line fixed rotating frame

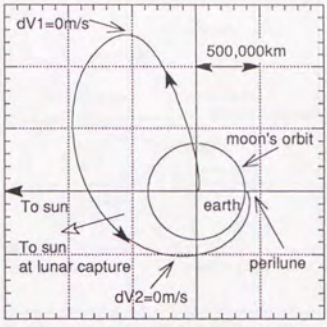

inertial frame

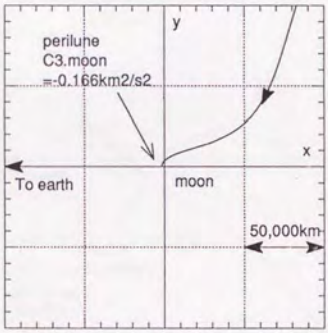

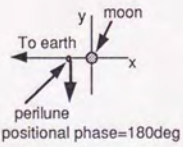

earth-moon-line fixed rotating frame

apogee distance 1,392,776 km
total flight time 101.82 day
dV1 = 0.06 m/s, dV2 = 0.03 m/s
C3 w.r.t. moon at perilune = - 0.166 km^2/s^2 (in-plane direct capture)

Fig.7-7 Orbital Profile (Orbit 2)

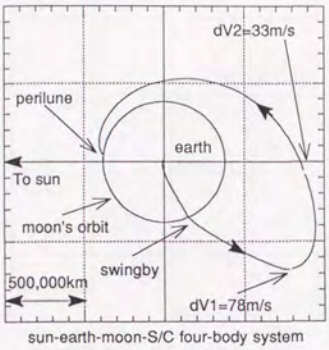

sun-earth-line fixed rotating frame

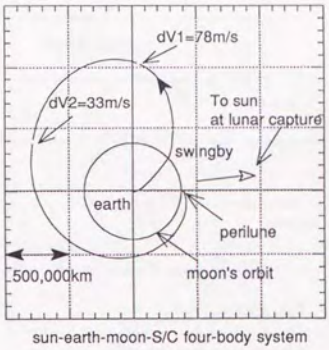

inertial frame

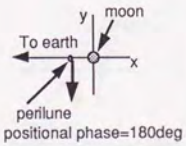

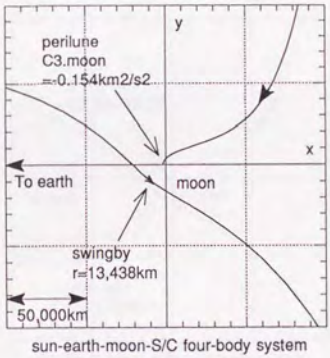

earth-moon-line fixed rotating frame

swingby distance	13,438 km
apogee distance	1,085,064 km
total flight time	81.47 day

dV1 = 78.0 m/s, dV2 = 33.2 m/s

C3 w.r.t. moon at perilune = - 0.154 km^2/s^2 (in-plane direct capture)

Fig.7-8 Orbital Profile (Orbit 3)

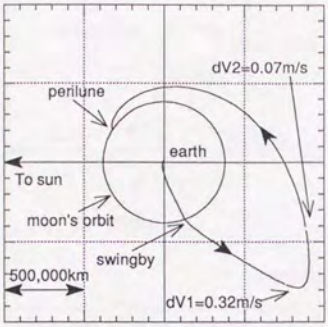

sun-earth-line fixed rotating frame

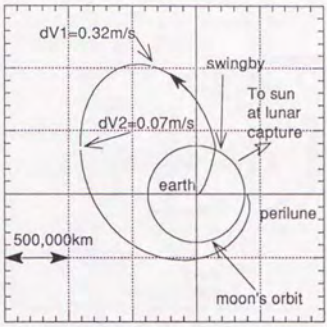

inertial frame

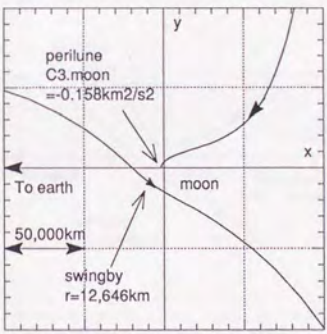

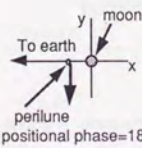

earth-moon-line fixed rotating frame

swingby distance	12,645 km
apogee distance	1,169,768 km
total flight time	79.63 day

dV1 = 0.32 m/s, dV2 = 0.07 m/s

C3 w.r.t. moon at perilune = - 0.158 km^2/s^2 (in-plane direct capture)

Fig.7-9 Orbital Profile (Orbit 4)

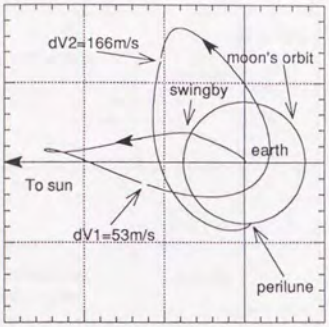

sun-earth-moon-S/C four-body system

sun-earth-line fixed rotating frame

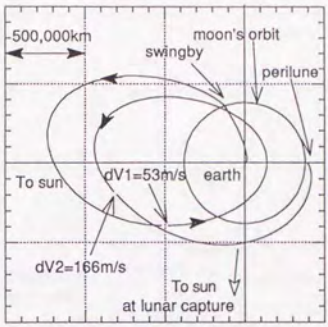

sun-earth-moon-S/C four-body system

inertial frame

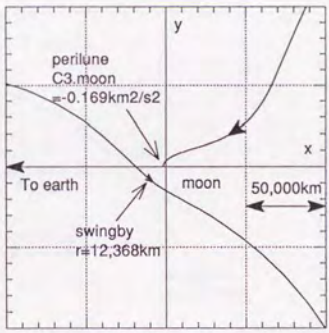

sun-earth-moon-S/C four-body system

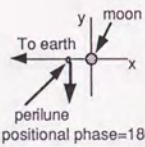

earth-moon-line fixed rotating frame

swingby distance	12,368 km
apogee distance	1,251,734km(1st), 947,869 km(2nd)
total flight time	131.16 day

dV1 = 53.6 m/s, dV2 = 165.8 m/s

C3 w.r.t. moon at perilune = - 0.169 km^2/s^2 (in-plane direct capture)

Fig.7-10 Orbital Profile (Orbit 5)

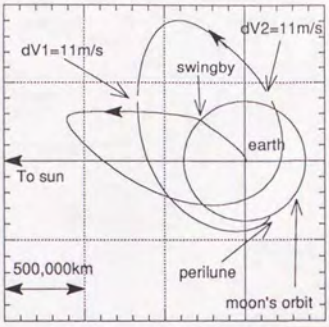

sun-earth-line fixed rotating frame

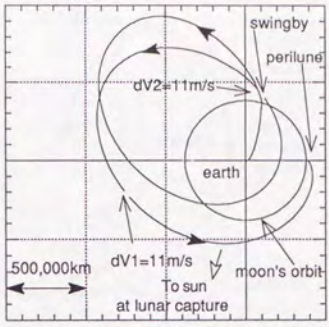

inertial frame

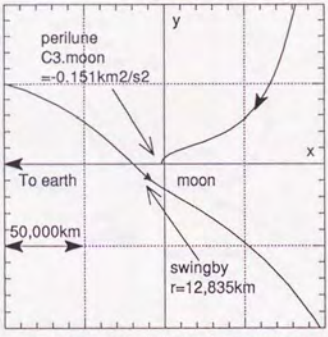

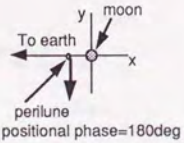

earth-moon-line fixed rotating frame

swingby distance	12,835 km
apogee distance	1,143,825km(1st), 1,012,337 km(2nd)
total flight time	133.80 day

dV1 = 10.7 m/s, dV2 = 10.9 m/s

C3 w.r.t. moon at perilune = - 0.151 km^2/s^2 (in-plane direct capture)

Fig.7-11 Orbital Profile (Orbit 6)

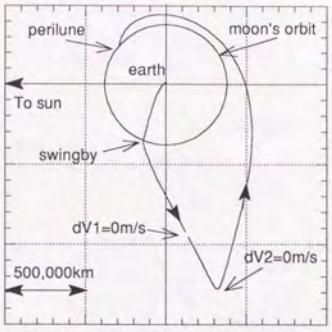

sun-earth-line fixed rotating frame

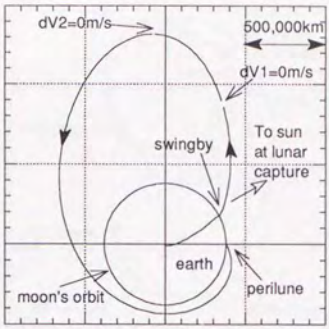

inertial frame

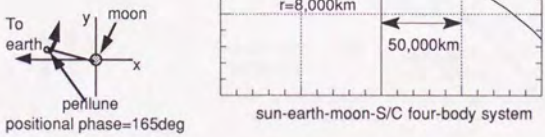

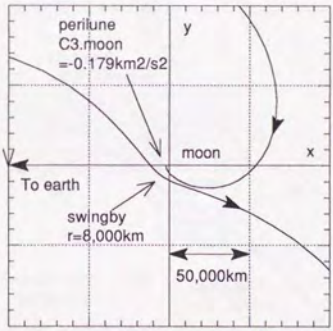

earth-moon-line fixed rotating frame

swingby distance	8,000 km
apogee distance	1,246,875km
total flight time	83.05 day

dV1 = 0.0 m/s, dV2 = 0.0 m/s

C3 w.r.t. moon at perilune = - 0.179 km^2/s^2 (in-plane retrograde capture)

Fig.7-12 Orbital Profile (Orbit 7)

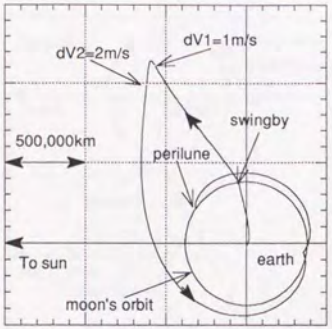

sun-earth-moon-S/C four-body system

sun-earth-line fixed rotating frame

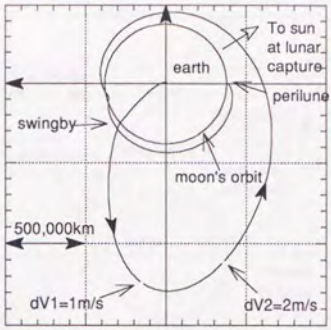

sun-earth-moon-S/C four-body system

inertial frame

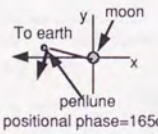

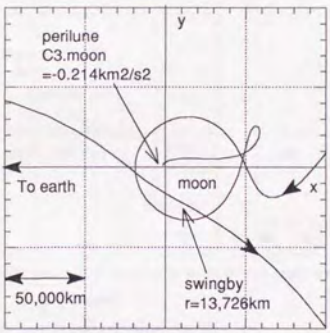

sun-earth-moon-S/C four-body system

earth-moon-line fixed rotating frame

swingby distance	13,726 km
apogee distance	1,291,270km
total flight time	95.05 day

dV1 = 1.1 m/s, dV2 = 1.9 m/s

C3 w.r.t. moon at perilune = - 0.214 km^2/s^2 (in-plane direct 'natural' capture)

Fig.7-13 Orbital Profile (Orbit 8)

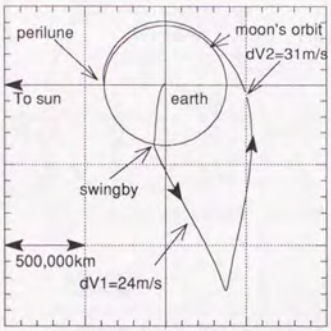

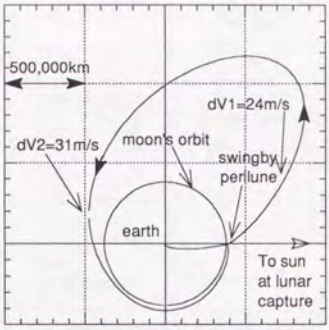

sun-earth-line fixed rotating frame　　inertial frame

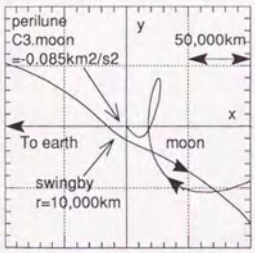

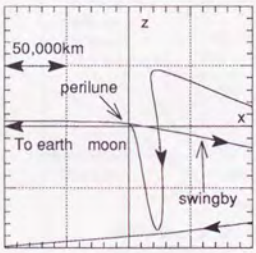

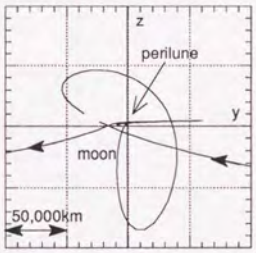

x-y plane　　x-z plane　　y-z plane

earth-moon-line fixed rotating frame

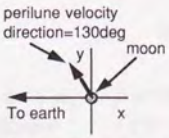

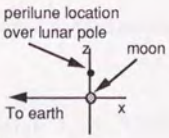

swingby distance	9,999 km
apogee distance	1,352,501 km
total flight time	84.9 day
midcourse delta-V	dV1 = 24.3 m/s, dV2 = 31.1 m/s

C3 w.r.t. moon at perilune = - 0.085 km^2/s^2 (polar capture)

Fig.7-14 Orbital Profile (Orbit 9)

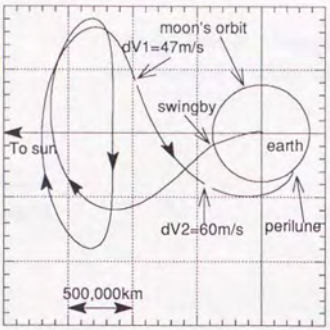

sun-earth-line fixed rotating frame

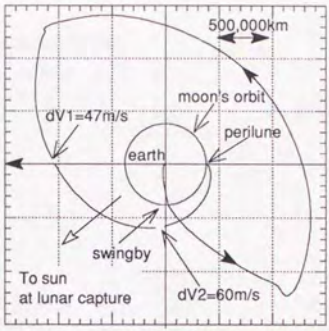

inertial frame

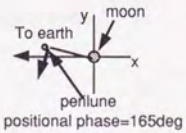

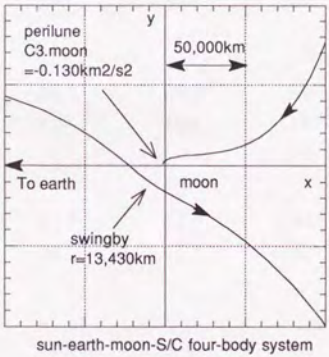

earth-moon-line fixed rotating frame

swingby distance	13,430 km
apogee distance	1,681,359km(1st), 1,710,777km(2nd), 1,709,575km(3rd)
total flight time	337.00 day

dV1 = 46.6 m/s, dV2 = 59.8 m/s

C3 w.r.t. moon at perilune = - 0.130 km^2/s^2 (in-plane direct capture)

Fig.7-15 Orbital Profile (Orbit 10)

Table 7-1 Orbital Sequences (orbit 1~orbit 5)

earth departure at 200km altitude circular orbit
lunar insertion at 100km altitude perilune

Orbit No.	1	2	3	4	5
Revolution No. around the earth	1	1	1	1	2
Swingby					
time(day)	-----	-----	2.9	2.8	3.0
swingby distance(km)	-----	-----	13,438	12,645	12,368
Midcourse delta-V					
time(day)	32.5	31.8	21.5	19.6	-----
geocentric distance(10^4km)	136	136	103	107	-----
1st apogee					
time(day)	40.4	40.5	30.9	31.5	38.0
geocentric distance(10^4km)	138	139	109	117	125
Midcourse delta-V					
time(day)	92.5	91.8	51.5	49.6	71.2
geocentric distance(10^4km)	54	54	87	97	66
2nd apogee					
time(day)	-----	-----	-----	-----	101.1
geocentric distance(10^4km)	-----	-----	-----	-----	95
Midcourse delta-V					
time(day)	-----	-----	-----	-----	111.2
geocentric distance(10^4km)	----	-----	-----	-----	83
C3 w.r.t. moon at perilune (km^2/s^2)	-0.165	-0.166	-0.154	-0.158	-0.169
Total flight time(day)	102.5	101.8	81.5	79.6	131.2

Table 7-1 Orbital Sequences (Cont., orbit 6~orbit 10)

earth departure at 200km altitude circular orbit
lunar insertion at 100km altitude perilune

Orbit No.	6	7	8	9	10
Revolution No. around the earth	2	1	1	1	(2)
Swingby					
time(day)	2.9	3.3	2.7	2.9	2.7
swingby distance(km)	12,835	8,000	13,726	10,000	13,430
Midcourse delta-V					
time(day)	-----	13.0	25.1	9.9	-----
geocentric distance(10^4km)	-----	94	125	83	-----
1st apogee					
time(day)	32.8	32.1	32.5	34.3	83.2
geocentric distance(10^4km)	114	125	129	135	168
Midcourse delta-V					
time(day)	73.8	33.0	45.1	70.0	-----
geocentric distance(10^4km)	43	132	117	51	-----
2nd apogee					
time(day)	95.8	-----	-----	-----	215.1, 235.0
geocentric distance(10^4km)	101	-----	-----	-----	171, 171
Midcourse delta-V					
time(day)	113.8	-----	-----	-----	307.0, 327.0
geocentric distance(10^4km)	78	-----	-----	-----	105, 59
C3 w.r.t. moon at perilune (km^2/s^2)	-0.151	-0.179	-0.214	-0.085	-0.130
Total flight time(day)	133.8	83.0	95.1	84.9	337.0

Table 7-2 Control Parameters (orbit 1~orbit 5)

	initial values		converged values
orbit 1 (five parameters)			
total flight time (day)	91.00000000000	--->	102.4623754967
perigee velocity (km/s)	10.97600000000	--->	10.96100326574
perigee positional phase*(deg)	0.000000000000	--->	-2.069316624121
perilune velocity(km/s)	2.271000000000	--->	2.273715189030
sun phase (deg)	284.0000000000	--->	334.5199310366
orbit 2 (five parameters)			
total flight time (day)	102.4623754967	--->	101.8226393154
perigee velocity (km/s)	10.96100326574	--->	10.96155893600
perigee positional phase*(deg)	-2.069316624121	--->	-2.140144319776
perilune velocity(km/s)	2.273715189030	--->	2.273547922620
sun phase (deg)	334.5199310366	--->	330.6500168868
orbit 3 (five parameters)			
total flight time (day)	71.45000000000	--->	81.46830054050
perigee velocity (km/s)	10.94800000000	--->	10.91906529792
perigee positional phase**(deg)	217.0000000000	--->	224.1162076621
perilune velocity(km/s)	2.271000000000	--->	2.276136217605
sun phase (deg)	112.0000000000	--->	172.9315129920
orbit 4 (five parameters)			
total flight time (day)	81.46830054050	--->	79.63447740564
perigee velocity (km/s)	10.91906529792	--->	10.91974266971
perigee positional phase**(deg)	224.1162076621	--->	224.1963985226
perilune velocity(km/s)	2.276136217605	--->	2.275270643666
sun phase (deg)	172.9315129920	--->	146.9058202842
orbit 5 (five parameters)			
total flight time (day)	130.0200000000	--->	131.1559378862
perigee velocity (km/s)	10.92000000000	--->	10.91599857060
perigee positional phase**(deg)	224.0000000000	--->	224.8490508696
perilune velocity(km/s)	2.275000000000	--->	2.272870181158
sun phase (deg)	260.0000000000	--->	275.5814753462

* in earth-moon fixed frame (measured from anti-earth direction)
** in sun-earth fixed frame (measured from anti-sun direction)

Table 7-2 Control Parameters (Cont., orbit 6~orbit 10)

	initial values		converged values
orbit 6 (five parameters)			
total flight time (day)	131.1559378862	--->	133.7990164752
perigee velocity (km/s)	10.91599857060	--->	10.91651861347
perigee positional phase**(deg)	224.8490508696	--->	224.6612070070
perilune velocity(km/s)	2.272870181158	--->	2.276922147800
sun phase (deg)	275.5814753462	--->	293.4721887222
orbit 7 (five parameters)			
total flight time (day)	79.63447740564	--->	83.04529163305
perigee velocity (km/s)	10.91974266971	--->	10.90828658585
perigee positional phase**(deg)	224.1963985226	--->	228.4349347552
perilune velocity(km/s)	2.271000000000	--->	2.270605105662
sun phase (deg)	146.9058202842	--->	141.6512135532
orbit 8 (five parameters)			
total flight time (day)	90.00000000000	--->	95.05061284180
perigee velocity (km/s)	10.91974266971	--->	10.92838606967
perigee positional phase**(deg)	224.1963985226	--->	222.8074401938
perilune velocity(km/s)	2.263000000000	--->	2.263038603500
sun phase (deg)	146.9058202842	--->	144.9935176422
orbit 9 (six parameters)			
total flight time (day)	71.45000000000	--->	84.85621334952
perigee velocity (km/s)	10.94800000000	--->	10.91919288213
perigee positional phase**(deg)	217.0000000000	--->	225.0762130555
perilune velocity(km/s)	2.295000000000	--->	2.291386553349
sun phase (deg)	112.0000000000	--->	179.3663976858
inclination at earth departure(deg)	0.000000000000	--->	4.494869940137
orbit 10 (five parameters)			
total flight time (day)	337.0000000000	--->	336.9999981607
perigee velocity (km/s)	10.92645660000	--->	10.92645658353
perigee positional phase**(deg)	222.9999747416	--->	222.9999822552
perilune velocity(km/s)	2.295000000000	--->	2.281514915287
sun phase (deg)	309.9765603397	--->	309.9765599648

* in earth-moon fixed frame (measured from anti-earth direction)
** in sun-earth fixed frame (measured from anti-sun direction)

Table 7-3 Performance Index (orbit 1~10)

Orbit 1				
	cost function	dV1+dV2		
	penalty function	apogee constraint	geocentric distance	1,380,000km,
			positional phase*	150deg
		swingby constraint	none	
Orbit 2				
	cost function	dV1+dV2		
	penalty function	apogee constraint	none	
		swingby constraint	none	
Orbit 3				
	cost function	dV1+dV2		
	penalty function	apogee constraint	geocentric distance	1,080,000km,
			positional phase*	331deg
		swingby constraint	lunicentric distance	8,900km
Orbit 4				
	cost function	dV1+dV2		
	penalty function	apogee constraint	none	
		swingby constraint	none	
Orbit 5				
	cost function	dV1+dV2		
	penalty function	apogee constraint	geocentric distance	880,000km,
			positional phase*	115deg (2nd apogee)
		swingby constraint	lunicentric distance	8,900km
Orbit 6				
	cost function	dV1+dV2		
	penalty function	apogee constraint	none	
		swingby constraint	none	
Orbit 7				
	cost function	dV1+dV2		
	penalty function	apogee constraint	none	
		swingby constraint	lunicentric distance	8,000km
Orbit 8				
	cost function	dV1+dV2		
	penalty function	apogee constraint	none	
		swingby constraint	none	
Orbit 9				
	cost function	dV1+dV2		
	penalty function	apogee constraint	none	
		swingby constraint	lunicentric distance	10,000km
Orbit 10				
	cost function	dV1+dV2		
	penalty function	apogee constraint	none	
		swingby constraint	none	

* positional phase in sun-earth fixed frame (measured from anti-sun direction)

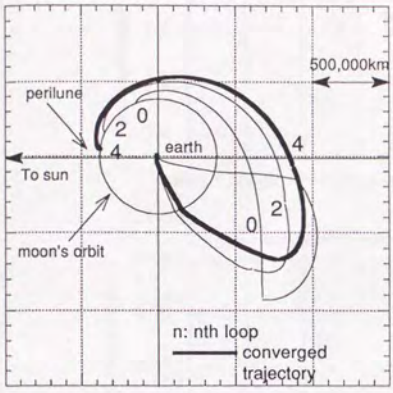

sun-earth-moon-S/C four-body system

orbit 3

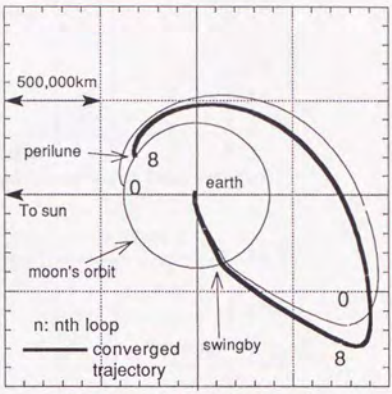

sun-earth-moon-S/C four-body system

orbit 4

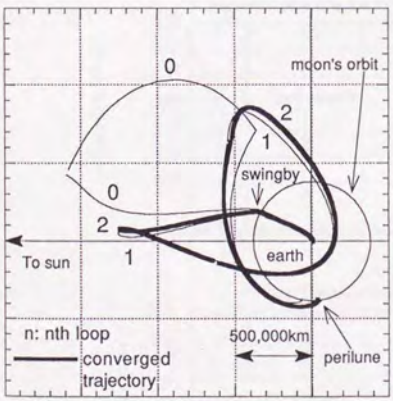

sun-earth-moon-S/C four-body system

orbit 5

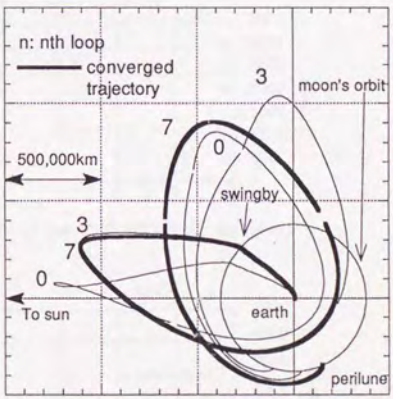

sun-earth-moon-S/C four-body system

orbit 6

Fig.7-16 Convergence of Trajecotry Design (orbit 3~6)

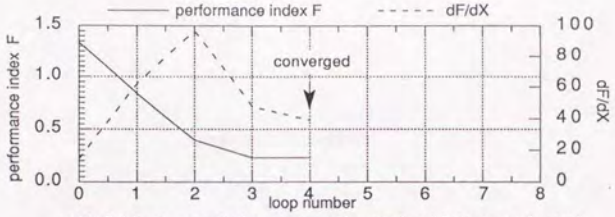

orbit 3 (single revolution around the earth with lunar swingby)

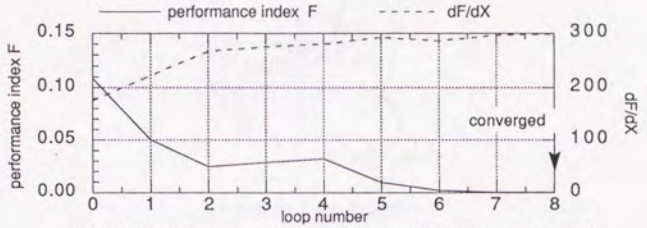

orbit 4 (single revolution around the earth with lunar swingby)

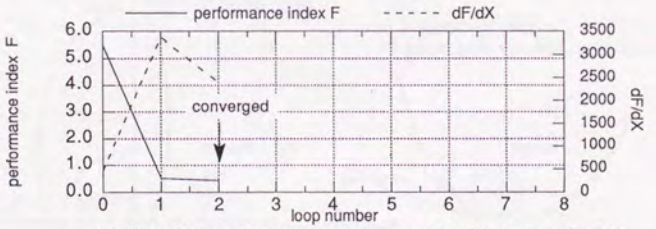

orbit 5 (double revolutions around the earth with lunar swingby)

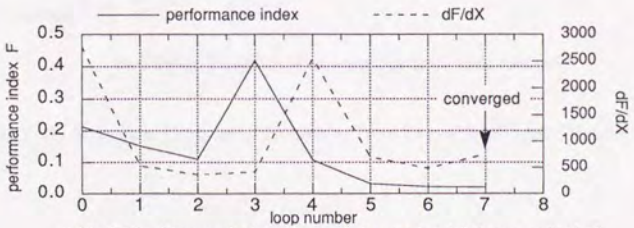

orbit 6 (double revolutions around the earth with lunar swingby)

Fig.7-17 Convergence of Performance Index (Orbit 3~6)

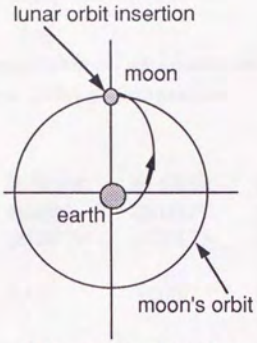

Hohmann Type Transfer

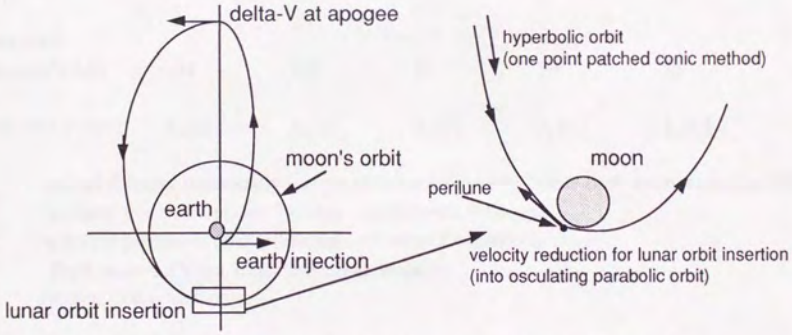

Bi-Elliptic Transfer (assuming patched conic method)

Fig.7-18 Schematic Diagram of Hohmann Transfer and Bi-Elliptic Transfer

Table 7-4 Conventional Transfer

earth departure at 200km altitude circular orbit
lunar insertion at 100km altitude perilune

	Hohmann transfer (Num. Int.*)	Hohmann transfer (PCM**)	Bi-elliptic transfer# (PCM**)	Bi-elliptic transfer## (PCM**)	Bi-parabolic transfer (PCM**)
earth injection (m/s)	3,116	3,131	3,200	3,223	3,224
delta-V at apogee (m/s)	-----	-----	281	17	0
lunar orbit insertion%(m/s)	134	145	15	36	38
total delta-V(m/s)	3,249	3,276	3,497	3,276	3,263

* optimal solution numerically integrated in earth-moon-S/C three-body system (see Fig.7-20)
(perigee positional phase=242deg, veloicty=10.900km/s,
perilune positional phase=240deg, velocity=2.4434km/s,
flight time=4.44days, direct motion at perilune)

** Patched Conic Method

\# apogee distance =1,500,000 km

apogee distance =28,200,000 km

% delta-V required for insertion into osculating parabolic orbit (C3 w.r.t. moon=0)

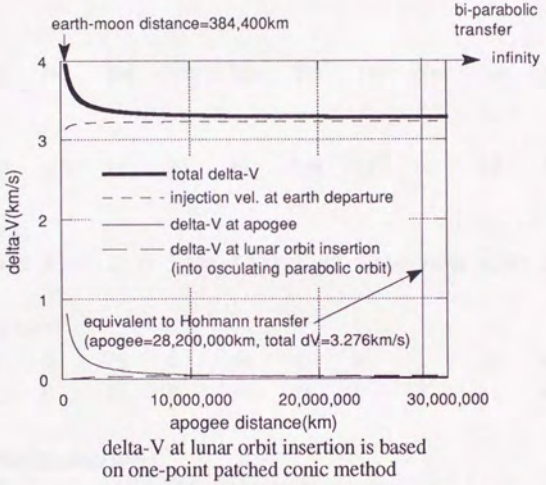

Fig.7-19 Effect of Apogee Distance on Bi-Elliptic Earth-Moon Transfer

Table 7-5 Total Velocity Correction

earth departure at 200km altitude circular orbit
lunar insertion at 100km altitude perilune

	Gravitational Capture										Hohmann*
Orbit No.	1	2	3	4	5	6	7	8	9	10	
Revolution No.around the Earth	1	1	1	1	2	2	1	1	1	2	-----
Swingby Use	No	No	Yes	Yes	Yes	Yes	Yes	Yes	Yes	Yes	-----
Flight time (day)	102	102	81	80	131	134	83	95	85	337	4.4
Earth Injection (m/s)	3,177	3,177	3,135	3,135	3,132	3,132	3,124	3,144	3,135	3,142	3,116
Midcourse delta-V (m/s)											
dV1	14	0	78	0	54	11	0	1	24	47	0
dV2	0	0	33	0	166	11	0	2	31	60	0
delta-V gain at lunar insertion (m/s)**	-36	-36	-34	-34	-37	-33	- 39	- 47	-18	- 28	+134
Total delta-V (m/s)	3,155	3,141	3,212	3,101	3,314	3,121	3,085	3,100	3,172	3,220	3,249
Comparison with Hohmann transfer (m/s)	- 94#	- 108	- 37#	- 148	+65#	- 129	- 165	- 149	- 78	- 29	0

* optimal case from viewpoint of total delta-V (see Table 7-6 and Fig.7-20)

** velocity gain under osculating parabolic velocity at lunar insertion (C3 w.r.t. moon=0)

\# Orbit 1, 3 and 5 are further optimized into orbit 2, 4 and 6 respectively by removing constraints.

Table 7-6 Velocity Gain Allotment in Earth-Moon Transfer with Gravitational Capture

earth departure at 200km altitude circular orbit
lunar insertion at 100km altitude perilune

	Hohmann transfer (Num. Int.*)	bi-elliptic transfer# (PCM**)	gravitational capture type transfer (Num. Int.***)	velocity gain allotment## Hohmann	bi-elliptic
earth injection (m/s)	3,116	3,200	3,135	lunar swingby and apogee distance combined effect +20	-65
delta-V at apogee (m/s)	-----	281	0	solar perturbation 0	-281
lunar orbit insertion%(m/s)	134	15	-34	gravitational capture -168	-49
total delta-V(m/s)	3,249	3,497	3,101	-148	-396

\# apogee distance =1,500,000 km

in comparison with Hohmann and bi-elliptic transfer

* optimal solution numerically integrated in earth-moon-S/C three-body system
(perigee positional phase=242deg, veloicty=10.900km/s,
perilune positional phase=240deg, velocity=2.4434km/s,
flight time=4.44days, direct capture at perilune)

** Patched Conic Method

*** numerical integration in sun-earth-moon-S/C four-body system (orbit 4)

% delta-V required for insertion into osculating parabolic orbit (C3 w.r.t. moon=0)

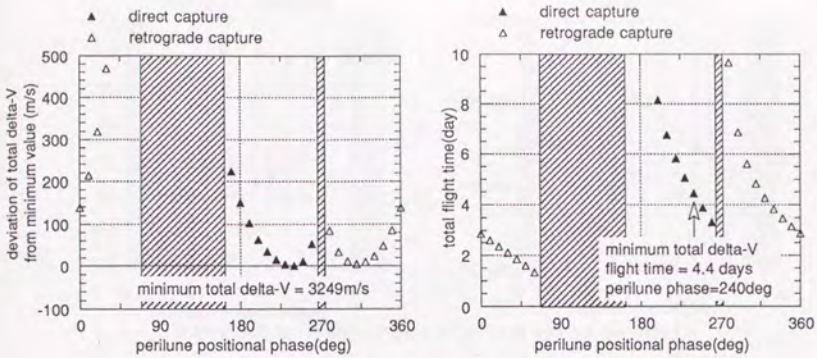

total delta-V　　flight time

assumptions

1) total delta-V = earth injection at 200km altitude circular orbit
+ lunar orbit insertion into osculating parabolic orbit at the altitude of 100km

2) numerical integration in earth-moon-S/C thre-body system

Fig.7-20 Effect of Perilune Location in Hohmann Transfer

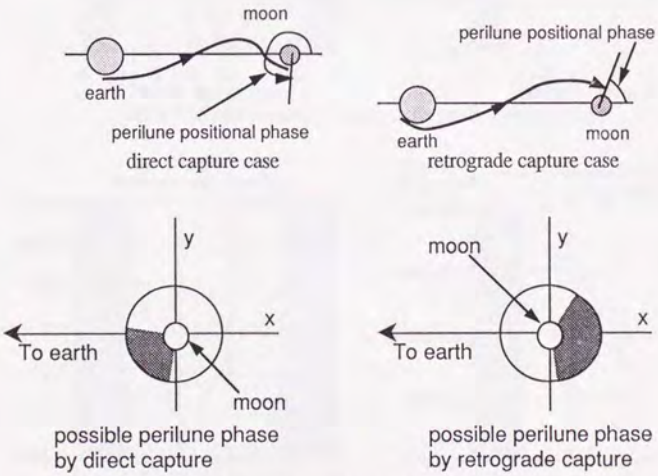

Fig.7-21 Perilune Phase Attainable in Hohmann Transfer

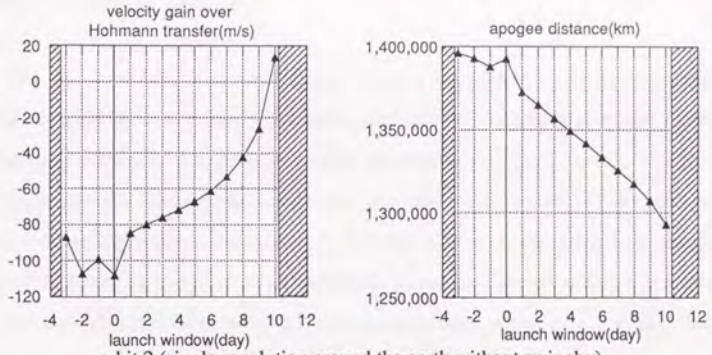

orbit 2 (single revolution around the earth without swingby)

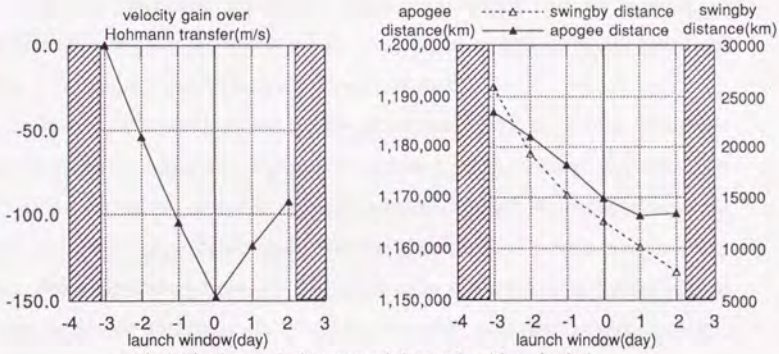

orbit 4 (single revolution around the earth with swingby)

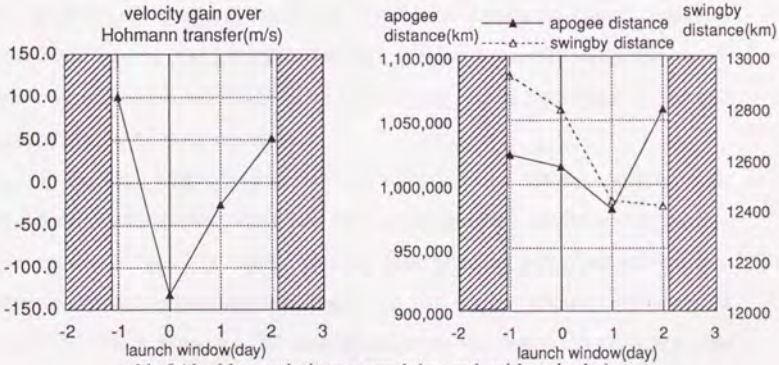

orbit 6 (double revolutions around the earth with swingby)

Fig.7-22 Launch Window Analysis

Chapter 8 Concluding Remarks

In this dissertation, 1) gravitational capture mechanism was revealed both analytically and numerically and 2) systematic procedure for its application to earth-moon transfer was established by positive use of solar perturbation.

Gravitational capture was defined as a phenomenon by which S/C can achieve elliptic osculating state at perilune (i.e. negative C3 w.r.t. the moon), although approaching from outside the sphere of influence. Its mechanism was analysed in terms of local C3 reduction in earth-moon-S/C three-body system, whose results predict that gravitational capture is classified into two categories: approach from earth side and from anti-earth side (Chapter 3). It was derived that outward force from the moon in the direction of earth-moon line due to moon's revolution around the earth (i.e. centrifugal force) is instrumental in reducing local C3 w.r.t. the moon.

Then, orbital profile in the vicinity of the moon prior to perilune arrival and resultant perilune conditions were numerically obtained, which confirmed the existence of both earth-side and anti-earth-side approach categories (Chapter 4). Furthermore, semi-major axis and perigee distance conditions prior to gravitational capture was concretely given: When approaching from earth side, semi-major axis and perigee distance prior to capture are around 200,000km and 100,000km, severally. As to anti-earth side approach, perigee distance is around earth-moon distance, while semi-major axis takes the value from 500,000km up to several million km. Satisfaction of these pre-capture conditions guarantees achievement of gravitational capture at moon. It was also shown that out-of-plane motion does not work in favor of gravitational capture mechanism in terms of reduction of local C3 w.r.t. the moon.

In the latter half, attention was paid to earth-moon transfer trajectory with gravitational capture at moon, which fully takes advantage of low relative velocity at lunar orbit insertion (Chapter 5). Firstly, possible solar effect to realize pre-gravitational capture conditions concerning semi-major axis and perigee distance was analyzed (Chapter 6). It was shown that S/C location in 2nd or 4th quadrant in geocentric sun-

earth fixed frame enhances local perigee distance mainly by decreasing local eccentricity, which yields that perigee distance may be enlarged from initially low earth orbit to finally earth-moon distance. This mechanism reveals the possibility of earth-moon transfer trajectory by positive use of solar perturbation. Based on this perigee raise dynamics, orbital profile of geocentric portion of earth-moon transfer was outlined in sun-earth-S/C three-body system in a quantitative way.

Furthermore, systematic orbit design methodology was newly proposed which effectively makes use of gravitational capture (Chapter 4) as well as solar effect analyses (Chapter 6). Underlying concept of the proposed method is parameter optimization problem, where midcourse velocity correction is taken into account (Chapter 7). Earth-moon transfer trajectory followed by gravitational capture was actually designed in multi-body system using the proposed method with satisfactory convergence. It was confirmed that analyses concerning gravitational capture (Chapter 4) and solar effect (Chapter 6) provide sufficient information for the initial guess in the proposed method.

Numerical examples show the feasibility of gravitational capture trajectory from flight time and delta-V point of view in comparison with conventional approaches such as Hohmann transfer and bi-elliptic transfer. Velocity gain of as much as 150 m/s can be obtained when compared with Hohmann-type transfer postulating lunar insertion point at 100km altitude. This corresponds to saving of 5% (9%) of S/C mass with specific impulse of 300 (180) seconds.

As noted in Chapter 2, MUSES-A spacecraft successfully reduced relative velocity with respect to the moon utilizing trajectory of the same kind in Oct., 1991 (i.e.swingby with low relative velocity [8]). With this experience, we consider that gravitational capture trajectory can be realized from navigational accuracy point of view and will contribute to lunar missions in the near future.

References

Lunar missions

1. R.Ridenoure,"Architecting a Mission Plan for Lunar Observer,"AAS-91-102, AAS/AIAA Space Flight Mechanics Meeting, Houston, Texas, 1991.

2. R.A.Cook, A.B.Sergeyevsky, E.A.Belbruno and T.H.Sweetser,"Return to the Moon: The Lunar Observer Mission,"AIAA-90-2888-CP, AIAA Astrodynamics Conference, Portland, Oregon, 1990.

3. R.J.Boain, "Small Lunar Missions," Japan-U.S. Joint Workshop on Missions to Near-Earth Objects Proceedings, November 21-22, 1991, Kyoto, pp.180-201.

4. K.Uesugi, T.Hayashi and H.Matsuo, "MUSES-A Double Lunar Swingby Mission," Acta Astronautica, Vol.17, No.5, 1988, pp.495-501.

5. K.Uesugi, J.Kawaguchi, S.Ishii, N.Ishii, M.Kimura and K.Tanaka, "Design of Double Lunar Swingby Orbits for MUSES-A and GEOTAIL,"AAS Paper 89-169-1, 1989.

6. K.Uesugi, H.Matsuo, J.Kawaguchi and T.Hayashi,"Japanese First Double Lunar Swingby Mission "HITEN","Acta Astronautica, Vol.25, No.7, 1991, pp.347-355.

7. K.Uesugi, J.Kawaguchi, N.Ishii, M.Shuto, M.Kamimura, N.Muranaka, M.Uo, M.Ogasawara, A.Kimura, S.Ishii, K.Tanaka, K.Shirakawa and M.Kimura,"Mission Operations of the Spacecraft HITEN,"3rd International Symposium on Spacecraft Flight Dynamics, September 30-Oct.4, Darmstadt, Germany, 1991.

8. K.Uesugi, J.Kawaguchi, N.Ishii, M.Shuto, H.Yamakawa and K.Tanaka, "Follow-on Mission Description of HITEN,"International Symposium on Space Technology and Science, May 17-23, Kagoshima, 1992.

9. K.Uesugi, J.Kawaguchi, N.Ishii, H.Yamakawa, M.Uo, H.Terada, M.Kimura and K.Shirakawa,"AOCS Operations of the Spacecraft GEOTAIL," Proceedings of 2nd Workshop on Astrodynamics and Flight Mechanics, Oct.5-6, Institute of Space and Astronautical Science, Sagamihara, 1992.

10. GORD (GEOTAIL Orbit Document), Rev.3.1, prepared by ISAS/GOOD (Institute of Space and Astronautical Science/Group of Orbit Design), June 5, 1992.

11. H.Mizutani, M.Kohno, S.Tsukamoto, J.Kawaguchi, H.Hinada and K.Ninomiya, "Lunar Interior Exploration by Lunar Penetrator Mission,"IAF 90-039, 41st Congress of the International Astronautical Federation, October 6-12, 1990, Dresden, GDR.

Possibility of capture in general three-body problem

12. H.Bondi,"Gravitational Capture,"Contemporary Physics, Vol.20, No.6, 1979, pp.585-591.

13. Y.Schmidt,"The Possibility of Capture in Celestial Mechanics,"Doklady Akademii Nauk SSSR, Vol.58, No.2, 1947, pp.213-216.

14. G.A.Merman,"On a Criterion for the Occurrence of a Hyperbolic-Elliptic Motion in the Problem of Three Bodies,"Doklady Akademii Nauk SSSR, Vol.85, No.4, 1952, p727-730.

15. K.A.Sitnikov,"The Possibility of Capture in the Problem of Three-Bodies," Doklady Akademii Nauk SSSR, Vol.87, No.4, 1952, p521-522.

16. G.F.Khil'mi, Qualitative Methods in the many-body problem, published by Gordon and Breach, New York, 1961.

17. V.M.Alekseev, "New Examples of Capture in the Three-Body Problem," Soviet Astronomy, Vol.6, No.4, 1963, pp.565-572.

Possibility of capture in restricted three-body problem

18. O.A.Sizova, "The Possibility of Capture in the Restricted Problem of Three Bodies," Doklady Akademii Nauk SSSR, Vol.86, No.3, 1952, pp.485-488.

19. G.A.Merman, "On Sufficient Conditions of Capture in the Restricted Hyperbolic Problem of Three Bodies with Close Binary Approaches," Byull. Inst. Teor. Astron., Vol.5, No.9, 1953, pp.325-372.

20. G.A.Merman, "The Restricted Parabolic Problem of Three Bodies," Byull. Inst. Teor. Astron., Vol.5, No.9, 1954, pp.606-616.

21. E.Hopf,"Zwei Satze uber den wahrscheinlichen Verlauf der Bewegungen dynamischer Systeme,"Mathematische Annalen, Vol.103, 1930, p710-719.

22. V.G.Fesenkov,"On the Possibility of Capture at Close Passages of Attracting Bodies,"Astronomicheskiy zhurnal, Akademii Nauk SSSR, (Astronomical Journal of the Soviet Union), Vol.23, No.1, 1946, pp.45-48.

23. V.A.Yegorov,"The Capture Problem in the Three-Body Restricted Orbital Problem,"NASA Technical Translation (TT) F-9, 1960, 16p.

24. Chao-Ho Sung,"The Possibility of Capture in the Restricted and in the General Problem of Three Bodies,"Ph.D Thesis, Yale University, 1969, 93p.

25. K.Tanikawa, Impossibility of the Capture of Retrograde Satellites in the Restricted Three-Body Problem," Celestial Mechanics, Vol.29, 1983, pp.367-402.

Satellite-aided capture

26. E.Everhart, "Close Encounters of Comets and Planets," The Astronomical Journal, Vol.74, No.5, 1969, pp.735-750.

27. O.Havnes,"The Capture of Comets by Jupiter,"Astrophysics and Space Science, Vol.5, 1969, pp.272-282.

28. E.Everhart, "The Origin of Short-Period Comets," Astrophysical Letters, Vo.10, 1972, pp.131-135.

29. Gp.Horedt,"Capture in the Restricted Three-Body Problem,"Acta Astronomica, Vol.22, No.1, 1972, pp.55-66.

30. E.Everhart, "Examination of Several Ideas of Comet Origin," The Astronomical Journal, Vol.78, No.4, 1973, pp.329-337.

31. Gp.Horedt,"Numerical Exploration of the Capture Problem,"Acta Astronomica, Vol.24, No.2, 1974, pp.207-213.

32. K.T.Nock and C.Uphoff,"Satellite-Aided Orbit Capture," AAS Paper 79-165, 1979, p.804, Abstract.

33. J.K.Cline,"Satellite Aided Capture," Celestial Mechanics, Vol.19, 1979, pp.405-415.

34. M.J.Valtonen and K.A.Innanen,"The Capture of Interstellar Comets," The Astronomical Journal, Vol.255, 1982, pp.307-315.

Analysis in circular and elliptic restricted three-body problem

35. J.M.Bailey,"Jupiter: Its Captured Satellites," Science, Vol.173, 1971, pp.812-813.

36. J.M.Bailey,"Origin of the Outer Satellites of Jupiter," Journal of Geophysical Research, Vol.76, No.32, 1971, pp.7827-7832.

37. J.M.Bailey,"Studies on Planetary Satellites. Satellite Capture in the Three-Body Elliptical Problem," The Astronomical Journal, Vol.77, No.2, 1972, pp.177-182.

38. T.A.Heppenheimer,"On the Presumed Capture Origin of Jupiter's Outer Satellites," Icarus, Vol.24, 1975, pp.172-180.

39. T.A.Heppenheimer and C.Porco,"New Contribution to the Problem of Capture," Icarus, Vol.30, 1977, pp.385-401.

40. J.Byl and M.W.Ovenden,"On the Satellite Capture Problem," Mon. Not. R. astr.Soc., Vol.173, 1975, pp.579-584.

41. R.J.Malcuit,"Numerical Simulation of Gravitational Capture of a Lunar-Like Body by Earth,"Proceedings of the 19th Lunar and Planetary Science Conference, 1989, pp.581-591.

42. V.Szebehely and R.T.Evans,"On the Capture of the Moon,"Celestial Mechanics, Vol.21, 1980, pp.259-264.

43. G.P.Horedt,"Capture of Planetary Satellites," The Astronomical Journal, Vol.81, No.8, 1976, pp.675-678.

44. R.B.Hunter, "Motions of Satellites and Asteroids under the Influence of Jupiter and the Sun I. Stable and Unstable Satellite Orbits," Mon.Not.R.astr.Soc., Vol.136, 1967, pp.245-265.

45. R.B.Hunter, "Motions of Satellites and Asteroids under the Influence of Jupiter and the Sun II. Asteroid Orbits Close to Jupiter," Mon.Not.R.astr.Soc., Vol.136, 1967, pp.267-277.

46. D.Benest, "Elliptic Restricted Problem for Sun-Jupiter: Existence of Stable Retrograde Satellites at Large Distance," Astron.& Astrophys. Vol.13, 1971, pp.157-160.

47. D.Benest, "Effects of the Mass Ratio on the Existence of Retrograde Satellites in the Circular Plane Restricted Problem," Astron.& Astrophys. Vol.32, 1974, pp.39-46.

48. T.Y.Huang and K.A.Innanen, "The Gravitational Escape/Capture of Planetary Satellites," The Astronomical Journal, Vol.88, No.10, 1983, pp.1537-1548.

49. M.Henon,"Numerical Exploration of the Restricted Problem.V.Hill's Case: Periodic Orbits and Their Stability," Astron.& Astrophys. Vol.1, 1969, pp.223-238.

50. M.Henon,"Numerical Exploration of the Restricted Problem.VI.Hill's Case: Non-Periodic Orbits," Astron.& Astrophys. Vol.9, 1970, pp.24-36.

51. R.Dvorak,"Critical Orbits in the Elliptic Restricted Three-Body Problem,"Astron.& Astrophys., Vol.167, 1986, pp.379-386.

52. D.Kotsakis,"Escapes and Captures,"Zeitschrift fur Astrophysik, Vol.69, 1968, pp.337-349.

53. M.A.Murison, "The Fractal Dynamics of Satellite Capture in the Circular Restricted Three-Body Problem," The Astronomical Journal, Vol.98, No.6, 1989, pp.2346-2359.

Application to earth-moon transfer

54. G.H.Darwin, "Periodic Orbits,"Acta Math., Vol.21, 1897, pp.99.

55. V.A.Yegorov, "Certain Problems of Moon Flight Dynamics," The Russian Literature of Satellites, Pt.1., Intern. Phys. Index, New York, 1958, pp.115.

56. B.Thuring, "Zwei Spezielle Mondeinfang-Bahnen in der Raumfahrt um Erde und Mond,"Astronaut. Acta, Vol.5, 1959, pp.241.

57. R.F.Arenstorf, "Existence of Periodic Solutions Passing near Both Masses of the Restricted Three-Body Problem,"AIAA Journal, Vol.1, 1963, pp.238.

58. M.C.Davidson, "Numerical Examples of Transition Orbits in the Restricted Three-Body System,"Astronomical Acta, Vol.10, 1964, pp.308-313.

59. C.C.Conley, "Low Energy Transit Orbits in the Restricted Three-Body Problem,"SIAM Journal.Appl.Math., Vol.16, No.4, 1968, pp.732-746.

60. T.A.Heppenheimer and D.Kaplan, "Guidance and Trajectory Considerations in Lunar Mass Transportation," AIAA Journal, Vol.15, No.4, 1977, pp.518-525.

61. T.A.Heppenheimer, "Achromatic Trajectories and Lunar Material Transport for Space Colonization," Journal of Spacecraft and Rockets, Vol.15, No.3, 1978, pp.176-183.

62. T.A.Heppenheimer, "A Mass-Catcher for Large-Scale Lunar Material Transport," Journal of Spacecraft and Rockets, Vol.15, No.4, 1978, pp.242-249.

63. T.A.Heppenheimer, "Steps Toward Space Colonization: Colony Location and Transfer Trajectories," Journal of Spacecraft and Rockets, Vol.15, No.5, 1978, pp.305-312.

64. E.A.Belbruno,"Lunar Capture Orbits, a Method of Constructing Earth Moon Trajectories and the Lunar Gas Mission,"AIAA-87-1054, 19th AIAA/DGLR /JSASS International Electric Propulsion Conference, Colorado Springs, Colorado, 1987.

65. E.A.Belbruno and J.K.Miller,"A Ballistic Lunar Capture Trajectory for the Japanese Spacecraft Hiten,"JPL IOM-90.4-1731, 1990.

66. E.A.Belbruno and J.K.Miller,"A Ballistic Lunar Capture Trajectory for the Lunar Observer Mission,"JPL IOM-90.4-1752, 1990.

67. J.K.Miller and E.A.Belbruno,"A Method for the Construction of a Lunar Transfer Trajectory Using Ballistic Capture,"AAS-91-100, AAS/AIAA Space Flight Mechanics Meeting, Houston, Texas, 1991.

68. T.Sweetser,"An Estimate of the Global Minimum dV Needed for Earth-Moon Transfer,"AAS-91-101, AAS/AIAA Space Flight Mechanics Meeting, Houston, Texas, 1991.

69. E.A.Belbruno and J.K.Miller,"Ballistic Lunar Capture Transfer by Utilization of Four-Body Perturbations with Two Applications,"submitted to publication of AIAA Journal of Guidance, Control and Navigation.

70. E.A.Belbruno, R.W.Ridenoure and J.Fernandez,"To the Moon from a B-52: Robotic Lunar Exploration Using the Pegasus Winged Rocket and Ballistic Lunar Capture,"5th Annual AIAA/Utah State University Conference on Small Satellites, Logan, Utah, 1991.

71. E.A.Belbruno,"Breakdown of Stable Motion and the Fuzzy Boundary in the Three-Dimensional Restricted Three-Body Problem with Applications," Private Memorandum, 1989.

72. E.A.Belbruno,"Examples of the Nonlinear Dynamics of Ballistic Capture and Escape in the Earth-Moon System,"AIAA-90-2896, AIAA Astrodynamics Conference, Portland, Oregon, 1990.

73. T.Tanabe,Y.Itoh,N.Ishii,and H.Yokota,"Visiting Libration Points in the Earth-Moon System Using a Lunar Swingby,"International Symposium on Space Technology and Science, Tokyo, 1982.

74. H.Yamakawa, J.Kawaguchi, N.Ishii and H.Matsuo,"Gravitational Capture Orbit in the Earth-Moon System," Proceedings of 1st Workshop on Astrodynamics and Flight Mechanics, pp.161-167, Dec.18-20, Institute of Space and Astronautical Science, Sagamihara, 1991.

75. H.Yamakawa, J.Kawaguchi, N.Ishii and H.Matsuo,"A Numerical Study of Gravitational Capture Orbit in the Earth-Moon System,"AAS-92-186, AAS/AIAA Spaceflight Mechanics Meeting, Colorado Springs, Colorado, Feb.24-26, 1992, also in Advances in the Astronautical Sciences, Vol.79, Part II, pp.1113-1132, Edited by R.E.Diehl, R.G.Schinnerer, W.E.Williamson and D.G.Boden.

76. H.Yamakawa, J.Kawaguchi, N.Ishii and H.Matsuo,"On Orbit Design Utilizing Lunar Gravitational Capture,"International Symposium on Space Technology and Science, May 17-23, Kagoshima, 1992.

77. H.Yamakawa, J.Kawaguchi, N.Ishii and H.Matsuo,"On Earth-Moon Transfer Trajectory Design with Gravitational Capture,"Proceedings of 2nd Workshop on Astrodynamics and Flight Mechanics, Oct.5-6, Institute of Space and Astronautical Science, Sagamihara, 1992.

General analysis of restricted three-body problem

78. V.Szebehely, Theory of Orbits, Academic Press, 1967.

Solar perturbation

79. B.D.Tapley and J.M.Lewallen,"Solar Influence on Satellite Motion Near the Stable Earth-Moon Libration Points," AIAA Journal, Vol.2, No.4, 1964, pp.728-732.

80. P.B.Richards, "Approximate Effect of the Sun on Satellites Near the Interior Earth-Moon Libration Point," AIAA Paper 65-512, AIAA Second Annual Meeting, San Francisco, California, 1965, 13p.

81. L.E.Wolaver,"Effect of Initial Configurations on Libration Point Motion," AIAA Paper 65-684, AIAA/ION Astrodynamics Specialist Conference, Monterey, California, 1965, 26p.

82. H.B.Schechter,"Three-Dimensional Nonlinear Stability Analysis of the Sun-Perturbed Earth-Moon Equilateral Points," AIAA Paper 67-566, AIAA Guidance, Control and Flight Dynamics Conference, Huntsville, Alabama, 1967, 7p.

83. F.T.Nicholson, "Effect of Solar Perturbations on Motion near the Collinear Earth-Moon Libration Points," AIAA Journal, Vol.5, No.12, 1967, pp.2237-2241.

84. H.B.Schechter,"Three-Dimensional Nonlinear Stability Analysis of the Sun-Perturbed Earth-Moon Equilateral Points," AIAA Journal, Vol.6, No.7, 1968, pp.1223-1228.

85. R.Kolenkiewicz and L.Carpenter, "Stable Periodic Orbits about the Sun-Perturbed Earth-Moon Triangular Points," AIAA Journal, Vol.6, No.7, 1968, pp.1301-1304.

86. D.Muhonen, S.Davis and D.Dunham, "Alternative Gravity-Assist Sequences for the ISEE-3 Escape Trajectory," AIAA Paper 84-1977, AIAA/AAS Astrodynamics Conference, Seattle, August 20-22, 1984, 9p.

Multi-swingby trajectory

87. H.Yokota,"Generation of Trajectories by Multiple Planetary Swingbys," Dr.Dissertation, University of Tokyo, 1982.

88. T.Hanyou,"Optimal Interplanetary Trajectory with Intermediate Impulses and Powered Swingbys --- with Emphasis on Jupiter Mission ---," Dr.Dissertation, University of Tokyo, 1986 (in Japanese).

89. L.A.D'Amario, D.V.Byrnes, L.Sackett and R.H.Stanford,"Optimization of Multiple Flyby Trajectories," AAS Paper 79-162, 1979, pp.695-729.

90. L.A.D'Amario, D.V.Byrnes and R.H.Stanford,"A New Method for Optimizing Multiple Flyby Trajectories," AIAA Paper 80-1676, AIAA/AAS Astrodynamics Conference, Danvers, Massachusetts, 1980, 8p.

Astrodynamics

91. F.W.Gobetz and J.R.Doll, "A Survey of Impulsive Trajectories," AIAA Journal, Vol.7, No.5, 1969, p.801.

92. R.H.Battin, Astronautical Guidance, McGraw-Hill, 1964.

93. A.B.Sergeyevsky, G.C.Snyder and R.A.Cunniff, Interplanetary Mission Design Handbook, Vol.1, Part 2, JPL Publications 82-43, 1983.

94. D.V.Byrnes and H.L.Cooper,"Multi-Conic: A Fast and Accurate Method of Computing Space Flight Trajectories," AIAA Paper 70-1062, AAS/AIAA Astrodynamics Conference, Santa Barbara, California, 1970, 8p.

Appendix A. Polar Coordinate Formulation of Three-Body System

Restricted three-body problem is formulated in polar coordinate with the smaller primary as origin. The earth and moon are postulated as two primary bodies. When sun-earth system is considered, the same derivation can be applied by exchanging gravity constant.

(1) Equations of Motion

Firstly, equations of motion are derived by use of Lagrangian formulation. In Fig.A-1, (ξ,η,ζ) coordinate denotes the inertial frame with the barycenter of the primaries as origin. On the other hand, (x,y,z) and (r,φ,χ) coordinates are defined in a rotating frame where positions of the primaries are fixed. In-plane positional phase φ is measured from anti-earth direction, while χ denotes elevation angle. Origin is situated at the barycenter of the primaries for (x,y,z) cartesian coordinate, while at the moon for (r,φ,χ) polar coordinate. Dimensionless mass of the earth and the moon is μ_1(=0.9878493317) and μ_2(=0.0121506683), respectively. The moon is assumed to orbit around the earth in circular motion with unit angular velocity i.e.$d\psi/dt=1$.

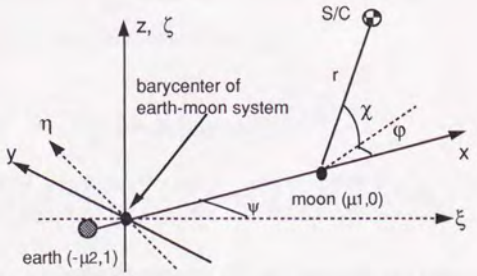

Fig.A-1 Restricted Three-Body Model (Cartesian and Polar Coordinate)

Transformation between three coordinates is expressed as shown below.

$$\begin{pmatrix}\xi\\ \eta\\ \zeta\end{pmatrix}=\begin{pmatrix}+\cos\psi & -\sin\psi & 0\\ +\sin\psi & +\cos\psi & 0\\ 0 & 0 & 1\end{pmatrix}\begin{pmatrix}x\\ y\\ z\end{pmatrix} \tag{A-1}$$

$$\begin{pmatrix}x\\ y\\ z\end{pmatrix}=\begin{pmatrix}\mu_1+r\cos\chi\cos\varphi\\ r\cos\chi\sin\varphi\\ r\sin\chi\end{pmatrix} \tag{A-2}$$

Using Eq.(A-1) and Eq.(A-2), kinetic energy T, potential energy U and velocity magnitude v in earth-moon-fixed rotating frame are now expressed in polar coordinate as follows;

$$\begin{aligned}T&=\frac{1}{2}\left(\left(\frac{d\xi}{dt}\right)^2+\left(\frac{d\eta}{dt}\right)^2+\left(\frac{d\zeta}{dt}\right)^2\right)\\ &=\frac{1}{2}\left(\left(\frac{dx}{dt}\right)^2+\left(\frac{dy}{dt}\right)^2+\left(\frac{dz}{dt}\right)^2\right)+\left(x\frac{dy}{dt}-\frac{dx}{dt}y\right)+\frac{1}{2}\left(x^2+y^2\right)\\ &=\frac{1}{2}\left(\left(\frac{dr}{dt}\right)^2+r^2\left(\frac{d\chi}{dt}\right)^2+r^2\left(\frac{d\varphi}{dt}\right)^2\cos^2\chi\right)\\ &\quad+r^2\frac{d\varphi}{dt}\cos^2\chi+\mu_1\left(\frac{dr}{dt}\cos\chi\sin\varphi-r\frac{d\chi}{dt}\sin\chi\sin\varphi+r\frac{d\varphi}{dt}\cos\chi\cos\varphi\right)\\ &\quad+\frac{1}{2}\left(\mu_1{}^2+2\mu_1 r\cos\chi\cos\varphi+r^2\cos^2\chi\right)\end{aligned} \tag{A-3}$$

$$U=-\frac{\mu_1}{r_1}-\frac{\mu_2}{r_2}=-\frac{\mu_1}{\left(1+r^2+2r\cos\chi\cos\varphi\right)^{1/2}}-\frac{\mu_2}{r} \tag{A-4}$$

$$v^2=\left(\frac{dx}{dt}\right)^2+\left(\frac{dy}{dt}\right)^2+\left(\frac{dz}{dt}\right)^2=\left(\frac{dr}{dt}\right)^2+r^2\left(\frac{d\chi}{dt}\right)^2+r^2\left(\frac{d\varphi}{dt}\right)^2\cos^2\chi \tag{A-5}$$

where r_1 and r_2 are distances between S/C and the earth and moon, respectively. Using Eq.(A-3) and Eq.(A-4), Lagrangian is derived in the following well-known form.

$$L = T - U \tag{A-6}$$

Equations of motion are derived from Eq.(A-3), Eq.(A-4) and Eq.(A-6) by Lagrange's formulation as follows;

$$\frac{d^2r}{dt^2} - r\left(\frac{d\chi}{dt}\right)^2 - r\left(\frac{d\varphi}{dt}\right)^2\cos^2\chi - 2r\frac{d\varphi}{dt}\cos^2\chi - \mu_1\cos\chi\cos\varphi - r\cos^2\chi + \frac{\mu_1(r+\cos\chi\cos\varphi)}{\left(1+r^2+2r\cos\chi\cos\varphi\right)^{3/2}} + \frac{\mu_2}{r^2} = 0 \tag{A-7}$$

$$2r\frac{dr}{dt}\frac{d\varphi}{dt}\cos^2\chi + r^2\frac{d^2\varphi}{dt^2}\cos^2\chi - 2r^2\frac{d\chi}{dt}\frac{d\varphi}{dt}\sin\chi\cos\chi + 2r\frac{dr}{dt}\cos^2\chi - 2r^2\frac{d\chi}{dt}\sin\chi\cos\chi + \mu_1 r\cos\chi\sin\varphi - \frac{\mu_1 r\cos\chi\sin\varphi}{\left(1+r^2+2r\cos\chi\cos\varphi\right)^{3/2}} = 0 \tag{A-8}$$

$$2r\frac{dr}{dt}\frac{d\chi}{dt} + r^2\frac{d^2\chi}{dt^2} + r^2\left(\frac{d\varphi}{dt}\right)^2\cos\chi\sin\chi + 2r^2\frac{d\varphi}{dt}\cos\chi\sin\chi + \mu_1 r\sin\chi\cos\varphi + r^2\cos\chi\sin\chi - \frac{\mu_1 r\sin\chi\cos\varphi}{\left(1+r^2+2r\cos\chi\cos\varphi\right)^{3/2}} = 0 \tag{A-9}$$

The same equations of motion are derived as long as the origin of the rotating frame (x,y,z) is located on the line connecting the two primaries.

(2) Jacobi Integral (Jacobi Constant)

Here, we define modified potential energy Ω as shown below.

$$\Omega = \frac{1}{2}\left(\mu_1+r\cos\chi\cos\varphi\right)^2 + \frac{1}{2}\left(r\cos\chi\sin\varphi\right)^2 + \frac{\mu_1}{(1+r^2+2r\cos\chi\cos\varphi)^{1/2}} + \frac{\mu_2}{r} + \frac{\mu_1\mu_2}{2} \tag{A-10}$$

Using Eq.(A-10), equations of motion Eq.(A-7) through Eq.(A-8) are transformed to as follows;

$$\frac{d^2r}{dt^2} - r\left(\frac{d\chi}{dt}\right)^2 - r\left(\frac{d\varphi}{dt}\right)^2\cos^2\chi - 2r\frac{d\varphi}{dt}\cos^2\chi = \frac{\delta\Omega}{\delta r} \qquad \text{(A-11)}$$

$$2r\frac{dr}{dt}\frac{d\varphi}{dt}\cos^2\chi + r^2\frac{d^2\varphi}{dt^2}\cos^2\chi - 2r^2\frac{d\chi}{dt}\frac{d\varphi}{dt}\sin\chi\cos\chi + 2r\frac{dr}{dt}\cos^2\chi - 2r^2\frac{d\chi}{dt}\sin\chi\cos\chi = \frac{\delta\Omega}{\delta\varphi} \qquad \text{(A-12)}$$

$$2r\frac{dr}{dt}\frac{d\chi}{dt} + r^2\frac{d^2\chi}{dt^2} + r^2\left(\frac{d\varphi}{dt}\right)^2\cos\chi\sin\chi + 2r^2\frac{d\varphi}{dt}\cos\chi\sin\chi = \frac{\delta\Omega}{\delta\chi} \qquad \text{(A-13)}$$

By use of Eq.(A-5), energy integral of Eq.(A-11) through Eq.(A-13) multiplied by dr/dt, dφ/dt and dχ/dt, respectively gives the following equation, where C is the integration constant,

$$\int\left(2\frac{dr}{dt}\frac{\delta\Omega}{\delta r} + 2\frac{d\varphi}{dt}\frac{\delta\Omega}{\delta\varphi} + 2\frac{d\chi}{dt}\frac{\delta\Omega}{\delta\chi}\right)dt = 2\Omega = v^2 + C \qquad \text{(A-14)}$$

which in turn gives,

$$\begin{aligned} C &= 2\Omega - v^2 \\ &= (\mu_1 + r\cos\chi\cos\varphi)^2 + (r\cos\chi\sin\varphi)^2 \\ &\quad + \frac{2\mu_1}{(1+r^2+2r\cos\chi\cos\varphi)^{1/2}} + \frac{2\mu_2}{r} + \mu_1\mu_2 - V^2 \end{aligned} \qquad \text{(A-15)}$$

This integration constant C is called Jacobi integral that stands for energy level in restricted three-body problem.

(3) C3 with Respect to the Moon and Earth

C_3, which is energy level in osculating state defined originally in inertial sense, is derived by use of polar coordinates. Differentiation of Eq.(A-1) yields the following equation describing S/C velocity in inertial frame;

$$\begin{pmatrix} \frac{d\xi}{dt} \\ \frac{d\eta}{dt} \\ \frac{d\zeta}{dt} \end{pmatrix} = \begin{pmatrix} +\frac{dx}{dt}\cos\psi - x\sin\psi - \frac{dy}{dt}\sin\psi - y\cos\psi \\ +\frac{dx}{dt}\sin\psi + x\cos\psi + \frac{dy}{dt}\cos\psi - y\sin\psi \\ \frac{dz}{dt} \end{pmatrix} \qquad \text{(A-16)}$$

On the other hand, position and velocity of two primaries in inertial frame are expressed as follows postulating their barycenter as origin (see Fig.A-1);

$$\begin{pmatrix} \xi_{moon} \\ \eta_{moon} \\ \zeta_{moon} \end{pmatrix} = \begin{pmatrix} +\mu_1\cos\psi \\ +\mu_1\sin\psi \\ 0 \end{pmatrix}, \quad \begin{pmatrix} d(\xi_{moon})/dt \\ d(\eta_{moon})/dt \\ d(\zeta_{moon})/dt \end{pmatrix} = \begin{pmatrix} -\mu_1\sin\psi \\ +\mu_1\cos\psi \\ 0 \end{pmatrix} \qquad \text{(A-17)}$$

$$\begin{pmatrix} \xi_{earth} \\ \eta_{earth} \\ \zeta_{earth} \end{pmatrix} = \begin{pmatrix} -\mu_2\cos\psi \\ -\mu_2\sin\psi \\ 0 \end{pmatrix}, \quad \begin{pmatrix} d(\xi_{earth})/dt \\ d(\eta_{earth})/dt \\ d(\zeta_{earth})/dt \end{pmatrix} = \begin{pmatrix} +\mu_2\sin\psi \\ -\mu_2\cos\psi \\ 0 \end{pmatrix} \qquad \text{(A-18)}$$

S/C's relative position and velocity with respect to the earth (r_E,V_E) and moon (r_M, V_M) in inertial frame are obtained by use of Eqs.(A-1) and (A-16)~(A-18) as follows;

$$r_E^2 = (x^2+y^2+z^2) + 2\mu_2 x + \mu_2^2 \qquad \text{(A-19)}$$

$$V_E^2 = \left(\frac{dx}{dt}\right)^2 + \left(\frac{dy}{dt}\right)^2 + \left(\frac{dz}{dt}\right)^2 + 2\left(x\frac{dy}{dt} - \frac{dx}{dt}y\right) + (x^2+y^2) + 2\mu_2\left(+x + \frac{dy}{dt}\right) + \mu_2^2 \qquad \text{(A-20)}$$

$$r_M^2 = (x^2+y^2+z^2) - 2\mu_1 x + \mu_1^2 \qquad \text{(A-21)}$$

$$V_M^2 = \left(\frac{dx}{dt}\right)^2 + \left(\frac{dy}{dt}\right)^2 + \left(\frac{dz}{dt}\right)^2 + 2\left(x\frac{dy}{dt} - \frac{dx}{dt}y\right) + (x^2+y^2) + 2\mu_1\left(-x - \frac{dy}{dt}\right) + \mu_1^2 \qquad \text{(A-22)}$$

Now we express C3 with respect to earth and moon (C3.earth and C3.moon) in polar coordinate formulation. Relation between cartesian and polar coordinate in primaries-fixed rotating frame is expressed by Eq.(A-2) and the following equation.

$$\begin{pmatrix} \frac{dx}{dt} \\ \frac{dy}{dt} \\ \frac{dz}{dt} \end{pmatrix} = \begin{pmatrix} \frac{dr}{dt}\cos\chi\cos\varphi - r\frac{d\chi}{dt}\sin\chi\cos\varphi - r\frac{d\varphi}{dt}\cos\chi\sin\varphi \\ +\frac{dr}{dt}\cos\chi\sin\varphi - r\frac{d\chi}{dt}\sin\chi\sin\varphi + r\frac{d\varphi}{dt}\cos\chi\cos\varphi \\ +\frac{dr}{dt}\sin\chi + r\frac{d\chi}{dt}\cos\chi \end{pmatrix} \quad \text{(A-23)}$$

Substituting Eqs.(A-2) and (A-23) into Eqs.(A-19)~(A-22) yields the next expressions.

$$r_M^2 = r^2 \quad \text{(A-24)}$$

$$V_M^2 = \left(\frac{dr}{dt}\right)^2 + r^2\left(\frac{d\chi}{dt}\right)^2 + r^2\left(\frac{d\varphi}{dt}\right)^2\cos^2\chi + 2r^2\frac{d\varphi}{dt}\cos^2\chi + r^2\cos^2\chi \quad \text{(A-25)}$$

$$r_E^2 = r^2 + 2r\cos\varphi + 1 \quad \text{(A-26)}$$

$$V_E^2 = \left(\frac{dr}{dt}\right)^2 + r^2\left(\frac{d\chi}{dt}\right)^2 + r^2\left(\frac{d\varphi}{dt}\right)^2\cos^2\chi + 2r^2\frac{d\varphi}{dt}\cos^2\chi + r^2\cos^2\chi + 1$$
$$+2\left(\frac{dr}{dt}\cos\chi\sin\varphi - r\frac{d\chi}{dt}\sin\chi\sin\varphi + r\cos\chi\cos\varphi + r\frac{d\varphi}{dt}\cos\chi\cos\varphi\right) \quad \text{(A-27)}$$

With Eqs.(A-24)-(A-27), C3.moon and C3.earth are derived as follows;

$$\text{C3.moon} = \left(\frac{dr}{dt}\right)^2 + r^2\left(\frac{d\chi}{dt}\right)^2 + r^2\left(\frac{d\varphi}{dt}\right)^2\cos^2\chi + 2r^2\frac{d\varphi}{dt}\cos^2\chi + r^2\cos^2\chi$$
$$-\frac{2\mu_2}{r} \quad \text{(A-28)}$$

$$C3.earth = \left(\frac{dr}{dt}\right)^2 + r^2\left(\frac{d\chi}{dt}\right)^2 + r^2\left(\frac{d\varphi}{dt}\right)^2\cos^2\chi + 2r^2\frac{d\varphi}{dt}\cos^2\chi + r^2\cos^2\chi + 1$$
$$+2\left(\frac{dr}{dt}\cos\chi\sin\varphi - r\frac{d\chi}{dt}\sin\chi\sin\varphi + r\cos\chi\cos\varphi + r\frac{d\varphi}{dt}\cos\chi\cos\varphi\right)$$
$$- \frac{2\mu_1}{(r^2+2r\cos\chi\cos\varphi+1)^{1/2}} \qquad \text{(A-29)}$$

(4) Conditions for Non-Positive C_3 with respect to Moon

Now, attention is paid to C_3 with respect to the moon. Non-positive C_3 conditions ($C3.moon \leq 0$) are obtained on various assumptions mainly for in-plane case.

a) General Case (In-plane motion)

The following non-positive C_3 condition is simply derived from Eq.(A-28) by assuming $\chi=0$ and $d\chi/dt=0$.

$$r^2\left(\frac{d\varphi}{dt}\right)\left(2+\frac{d\varphi}{dt}\right) \leqq -\left(\frac{dr}{dt}\right)^2 - \left(r^2 - \frac{2\mu_2}{r}\right) \qquad \text{(A-30)}$$

When r is greater than $(2\mu_2)^{1/3}$, the second term on the right side becomes negative so that angular velocity $d\varphi/dt$ is restricted to as follows;

$$-2 \leqq \frac{d\varphi}{dt} \leqq 0 \qquad \text{(A-31)}$$

These observation yields the following proposition, where the value $(2\mu_2)^{1/3}$ is defined as critical distance, which is 111,342 km in the earth-moon system.

Proposition A-1 Direct in-plane motion orbit ($d\varphi/dt>0$) does not exist under non-positive C_3 condition, in case distance from the moon exceeds the critical distance $(2\mu_2)^{1/3}$.

END

b) Zero Radial Velocity Case (In-plane motion assuming dr/dt=0)

Equation below states the non-positive C_3 condition which corresponds to the periapsis passage i.e. dr/dt=0. Similarly to the general case stated above, when distance from the moon surpasses the critical distance $(2\mu_2)^{1/3}$, no direct motion orbit ($d\varphi/dt>0$) exists, as maximum value of angular component becomes negative.

$$-r-\sqrt{\frac{2\mu_2}{r}} \leqq r\frac{d\varphi}{dt} \leqq -r+\sqrt{\frac{2\mu_2}{r}}. \qquad \text{(A-32)}$$

c) Zero Total Velocity Case (cusps where dr/dt=0, $d\varphi/dt=0$ and $d\chi/dt=0$)

Zero total velocity in earth-moon fixed rotating frame (i.e.v=0) would form a cusp in the orbital shape, while C_3 with respect to the moon becomes a function of only distance from the moon. Thus the following propositions are derived.

Proposition A-2 At cusps (where v=0) located over lunar pole (χ=90 deg), C3 w.r.t. the moon is always negative, as seen from the equation below derived from Eq.(A-28).

$$C3.moon = -\frac{2\mu_2}{r} \qquad \text{(A-33)}$$

END

Proposition A-3 At cusps (where v=0) located on the plane defined by the primaries' motion (χ=0), lunicentric distance below the critical distance $(2\mu_2)^{1/3}$ always results in non-positive C3 w.r.t. the moon (see Eq.(A-34) and Fig.A-2)).

$$C3.moon \leqq 0 \text{ if } r \leqq \sqrt[3]{2\mu_2},$$
$$C3.moon > 0 \text{ if } r > \sqrt[3]{2\mu_2}. \qquad \text{(A-34)}$$

END

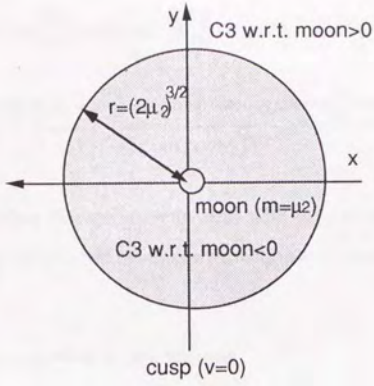

Fig.A-2 Cusp Location

(5) Time Derivative of C_3 with Respect to the Moon

Differentiation of Eq.(A-28) with respect to time yields the following Eq.(A-35).

$$\frac{d(C3.moon)}{dt} = 2\frac{dr}{dt}\frac{d^2r}{dt^2} + 2r\frac{dr}{dt}\left(\frac{d\chi}{dt}\right)^2 + 2r^2\frac{d\chi}{dt}\left(\frac{d^2\chi}{dt^2}\right) + 2r\frac{dr}{dt}\left(\frac{d\varphi}{dt}\right)^2\cos^2\chi$$
$$+ 2r^2\frac{d\varphi}{dt}\frac{d^2\varphi}{dt^2}\cos^2\chi - 2r^2\frac{d\chi}{dt}\left(\frac{d\varphi}{dt}\right)^2\cos\chi\sin\chi + 4r\frac{dr}{dt}\frac{d\varphi}{dt}\cos^2\chi$$
$$+ 2r^2\frac{d^2\varphi}{dt^2}\cos^2\chi - 4r^2\frac{d\chi}{dt}\frac{d\varphi}{dt}\cos\chi\sin\chi + 2r\frac{dr}{dt}\cos^2\chi$$
$$- 2r^2\frac{d\chi}{dt}\cos\chi\sin\chi + \frac{2\mu_2}{r^2}\frac{dr}{dt} \qquad \text{(A-35)}$$

Substitution of d^2r/dt^2, $d^2\varphi/dt^2$ and $d^2\chi/dt^2$ derived from equations of motion, Eqs.(A-7)~Eq.(A-9), transforms Eq.(A-35) into the following form. This operation is equivalent to the use of constancy of Jacobi integral as seen from the derivation of Eq.(A-15).

$$\frac{d(C3.moon)}{dt} = 2\mu_1\left(\left(\frac{dr}{dt}\cos\chi\cos\varphi - r\frac{d\varphi}{dt}\cos\chi\sin\varphi - r\cos\chi\sin\varphi - r\frac{d\chi}{dt}\sin\chi\cos\varphi\right)\right.$$

$$\left. + \frac{\left(-r\frac{dr}{dt} - \frac{d\,r}{dt}\cos\chi\cos\varphi + r\frac{d\varphi}{dt}\cos\chi\sin\varphi + r\cos\chi\sin\varphi + r\frac{d\chi}{dt}\sin\chi\cos\varphi\right)}{\left(1+r^2+2r\cos\chi\cos\varphi\right)^{3/2}}\right) \qquad \text{(A-36)}$$

Here, we postulate that the analysis deals with the regions in the vicinity of the moon. On this assumption, the following approximation as a result of Taylor expansion is used.

$$(1+r^2+2r\cos\chi\cos\varphi)^{-3/2} = 1 - 3r\cos\chi\cos\varphi \qquad \text{(A-37)}$$

where the power of S/C-moon distance higher than the second order i.e.r^n (n=2,3,...) is ignored. Substitution of Eq.(A-37) for Eq.(A-36) yields,

$$\frac{d(C3.moon)}{dt} = 2\mu_1 r\frac{dr}{dt}\left(3\cos^2\chi\cos^2\varphi - 1\right) \qquad \text{(A-38)}$$

Note that Eq.(A-38) is independent of the direction of revolution around the moon, that is $d\varphi/dt$ and $d\chi/dt$. From Eq.(A-38), the following propositions are derived.

Proposition A-4 Suppose that S/C is approaching the moon ($dr/dt<0$ and $r<<1$) in planar motion ($\chi=0$). Then C_3 with respect to the moon decreases ($d(C3.moon)/dt<0$), if the positional phase φ in the earth-moon fixed rotating frame satisfies the following conditions (see Fig.A-3).

$$-\varphi_0 \leqq \varphi \leqq +\varphi_0 \quad \text{or} \quad \pi-\varphi_0 \leqq \varphi \leqq \pi+\varphi_0$$

$$\text{where } \varphi_0 = \cos^{-1}\left(\frac{1}{\sqrt{3}}\right) = 54.74 \text{ deg} \qquad \text{(A-39)}$$

END

The proposition above predicts that gravitational capture orbit, which requires C_3 to be finally negative at perilune, tends to approach the moon from the earth side or anti-earth side.

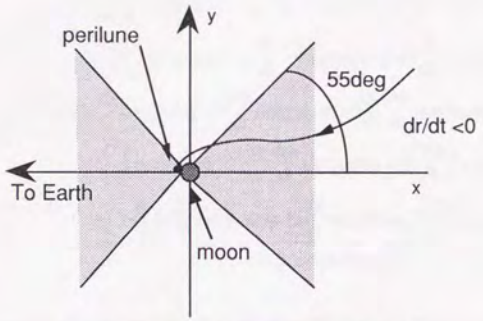

Fig.A-3 Regions for d(C3.moon)/dt < 0

Proposition A-5 Suppose that S/C is approaching the moon (dr/dt<0 and r<<1). Then it is derived that out-of-plane motion does not work in favor of reduction in C_3 with respect to the moon, since magnitude of the right side of Eq.(A-38), concerning d(C3.moon)/dt, decreases in accordance with out-of-plane displacement ($\cos\chi$) if lunicentric distance r and in-plane position φ are constant.

END

(6) Time Derivative of C_3 with Respect to the Earth

Differentiation of Eq.(A-29) with respect to time yields,

$$\frac{d(C3.earth)}{dt} = +2\frac{dr}{dt}\frac{d^2r}{dt^2} +2r\frac{dr}{dt}\left(\frac{d\chi}{dt}\right)^2 +2r^2\frac{d\chi}{dt}\frac{d^2\chi}{dt^2} +2r\frac{dr}{dt}\left(\frac{d\varphi}{dt}\right)^2\cos^2\chi$$
$$+2r^2\frac{d\varphi}{dt}\frac{d^2\varphi}{dt^2}\cos^2\chi -2r^2\frac{d\chi}{dt}\left(\frac{d\varphi}{dt}\right)^2\cos\chi\sin\chi + 4r\frac{dr}{dt}\left(\frac{d\varphi}{dt}\right)\cos^2\chi$$

$$+2r^2\frac{d^2\varphi}{dt^2}\cos^2\chi - 4r^2\frac{d\chi}{dt}\frac{d\varphi}{dt}\cos\chi\sin\chi + 2r\frac{dr}{dt}\cos^2\chi$$
$$- 2r^2\frac{d\chi}{dt}\cos\chi\sin\chi + 2\frac{d^2r}{dt^2}\cos\chi\sin\varphi - 2\frac{dr}{dt}\frac{d\chi}{dt}\sin\chi\sin\varphi$$
$$+2\frac{dr}{dt}\frac{d\varphi}{dt}\cos\chi\cos\varphi - 2\frac{dr}{dt}\frac{d\chi}{dt}\sin\chi\sin\varphi - 2r\frac{d^2\chi}{dt^2}\sin\chi\sin\varphi$$
$$-2r\left(\frac{d\chi}{dt}\right)^2\cos\chi\sin\varphi - 2r\frac{d\varphi}{dt}\frac{d\chi}{dt}\sin\chi\cos\varphi + 2\frac{dr}{dt}\cos\chi\cos\varphi$$
$$-2r\frac{d\chi}{dt}\sin\chi\cos\varphi - 2r\frac{d\varphi}{dt}\cos\chi\sin\varphi + 2\frac{dr}{dt}\frac{d\varphi}{dt}\cos\chi\cos\varphi$$
$$+2r\frac{d^2\varphi}{dt^2}\cos\chi\cos\varphi - 2r\frac{d\chi}{dt}\frac{d\varphi}{dt}\sin\chi\cos\varphi - 2r\left(\frac{d\varphi}{dt}\right)^2\cos\chi\sin\varphi$$
$$+\frac{\mu_1\left[2r\frac{dr}{dt}+2\frac{dr}{dt}\cos\chi\cos\varphi-2r\frac{d\chi}{dt}\sin\chi\cos\varphi-2r\frac{d\varphi}{dt}\cos\chi\sin\varphi\right]}{\left[1+r^2+2r\cos\chi\cos\varphi\right]^{3/2}} \qquad \text{(A-40)}$$

Substitution of d^2r/dt^2, $d^2\varphi/dt^2$ and $d^2\chi/dt^2$ derived from equations of motion, Eq.(A-7)~(A-9), transforms Eq.(A-40) into the following simple form.

$$\frac{d(C3.earth)}{dt} = 2\mu_2\left[-\frac{\frac{dr}{dt}+\cos\chi\sin\varphi}{r^2}\right]$$
$$+2\mu_2\left[r\frac{d\varphi}{dt}\cos\chi\sin\varphi - \frac{dr}{dt}\cos\chi\cos\varphi + r\cos\chi\sin\varphi + r\frac{d\chi}{dt}\sin\chi\cos\varphi\right] \qquad \text{(A-41)}$$

When in the vicinity of the moon ($r \ll 1$), Eq.(A-41) is approximated as follows since the first term on the right side becomes overwhelming;

$$\frac{d(C3.earth)}{dt} = 2\mu_2\left[-\frac{\frac{dr}{dt}+\cos\chi\sin\varphi}{r^2}\right] \qquad \text{(A-42)}$$

Now, condition for C3 w.r.t. earth reduction is investigated using Eq.(A-42) assuming in-plane motion ($\cos\chi=1$). Negative derivative of C3 w.r.t. earth ($d(C3.earth)/dt<0$) requires summation of derivative of lunicentric distance (dr/dt) and sine

of positional phase (sinφ) to be positive. As far as S/C approaches the moon, derivative of lunicentric distance (dr/dt) is negative. Thus, the following proposition is derived.

Proposition A-6 Assume that S/C is approaching the moon in planar motion (dr/dt<0, r<<1 and χ=0). Then, as far as local C_3 with respect to the earth decreases, positional phase φ in the earth-moon fixed rotating frame is restricted to the region ahead of moon's motion (0<φ<180deg).

END

(7) Angular Momentum around the Moon and Earth

Next, angular momentum w.r.t. the primaries is derived in polar coordinates focusing on in-plane motion. With Eq.(A-1) and Eq.(A-16)~(A-18), first, angular momentum around the axis perpendicular to the plane defined by the primaries' motion is expressed by cartesian cooridnate as follows;

$$h.moon = -y\frac{dx}{dt}+x^2 - 2\mu_1 x+x\frac{dy}{dt} - \mu_1\frac{dy}{dt}+y^2+\mu_1{}^2 \quad (A\text{-}43)$$

$$h.earth = -y\frac{dx}{dt}+x^2 + 2\mu_2 x+x\frac{dy}{dt} + \mu_2\frac{dy}{dt}+y^2+\mu_2{}^2 \quad (A\text{-}44)$$

Substitution of Eq.(A-2) and Eq.(A-23) assuming $\chi=d\chi/dt=0$ into Eqs.(A-43) and (A-44) yields the following.

$$h.moon = r^2 + r^2\frac{d\varphi}{dt} \quad (A\text{-}45)$$

$$h.earth = 1+2r\cos\varphi+\frac{dr}{dt}\sin\varphi+r\frac{d\varphi}{dt}\cos\varphi+r^2+r^2\frac{d\varphi}{dt} \quad (A\text{-}46)$$

(8) Time Derivative of Angular Momentum around the Moon and Earth

Differentiation of Eq.(A-45) and Eq.(A-46) yields,

$$\frac{d(h.moon)}{dt} = 2r\frac{dr}{dt} + 2r\frac{dr}{dt}\frac{d\varphi}{dt} + r^2\frac{d^2r}{dt^2} \qquad \text{(A-47)}$$

$$\frac{d(h.earth)}{dt} = 2\frac{dr}{dt}\cos\varphi - 2r\frac{d\varphi}{dt}\sin\varphi + \frac{d^2r}{dt^2}\sin\varphi + 2\frac{dr}{dt}\frac{d\varphi}{dt}\cos\varphi$$
$$+ r\frac{d^2\varphi}{dt^2}\cos\varphi - r\left(\frac{d\varphi}{dt}\right)^2\sin\varphi + 2r\frac{dr}{dt}\frac{d\varphi}{dt} + r^2\frac{d^2\varphi}{dt^2} + 2r\frac{dr}{dt} \qquad \text{(A-48)}$$

By use of equations of motion, Eqs.(A-7)~(A-9), Eq.(A-47) and Eq.(A-48) are transformed into the following form.

$$\frac{d(h.moon)}{dt} = -\mu_1 r\sin\varphi\left[1 - \frac{1}{(1+r^2+2r\cos\varphi)^{3/2}}\right] \qquad \text{(A-49)}$$

$$\frac{d(h.earth)}{dt} = -r\sin\varphi + \mu_2\sin\varphi\left[2r - \frac{1}{r^2}\right] \qquad \text{(A-50)}$$

From Eqs.(A-49) and (A-50), the following proposition can be found.

Proposition A-7 Concerning both primaries, derivative of angular momentum is a function of S/C position in earth-moon fixed frame and is independent of velocity.

END

Appendix B. Cartesian Coordinate Formulation of Three-Body System (Rotating Frame)

Restricted three-body problem is formulated by use of cartesian coordinate in rotating frame where positions of the primaries are fixed. Two primary bodies are assumed to be constituted of the earth and moon.

(1) Equations of Motion

In Fig.B-1, (ξ,η,ζ) denotes inertial frame, while (x,y,z) is primaries-fixed rotating frame with barycenter of two primaries as origin. In each frame, ζ (z) axis is defined so that it constitutes right-hand system. In the adopted model, the moon is assumed to orbit around the earth in circular motion. Mass of the earth and the moon is μ_1(=0.9878493317) and μ_2(=0.0121506683) respectively, whose positions are fixed at $(-\mu_2,0,0)$ and $(\mu_1,0,0)$ under normalization.

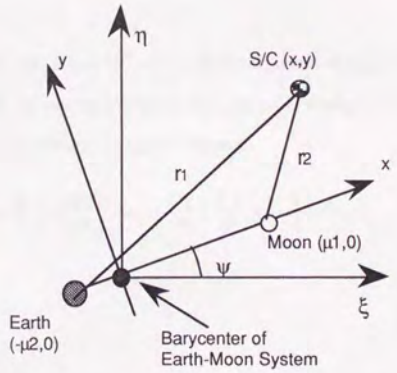

Fig.B-1 Restricted Three-Body Model (Cartesian Coordinate)

The transformation between (x,y,z) and (ξ,η,ζ) coordinates is expressed as follows;

$$\begin{pmatrix} \xi \\ \eta \\ \zeta \end{pmatrix} = \begin{pmatrix} +\cos\psi & -\sin\psi & 0 \\ +\sin\psi & +\cos\psi & 0 \\ 0 & 0 & 1 \end{pmatrix} \begin{pmatrix} x \\ y \\ z \end{pmatrix} \qquad \text{(B-1)}$$

For the derivation of equations of motion, we use Lagrange's formulation. Lagrangian is shown below in the well-known form.

$$L = T - U \qquad \text{(B-2)}$$

where T is kinetic energy and U is potential energy as follows;

$$T = \frac{1}{2}\left(\left(\frac{d\xi}{dt}\right)^2 + \left(\frac{d\eta}{dt}\right)^2 + \left(\frac{d\zeta}{dt}\right)^2\right) \qquad \text{(B-3)}$$

$$U = -\frac{\mu_1}{r_1} - \frac{\mu_2}{r_2} \qquad \text{(B-4)}$$

r_1 and r_2 is S/C-earth and S/C-moon distance, respectively. By virtue of coordinate transformation, Eq.(B-1), kinetic energy T and potential energy U are expressed in earth-moon fixed cartesian coordinate (x,y,z) as follows;

$$T = \frac{1}{2}\left(\left(\frac{dx}{dt}\right)^2 + \left(\frac{dy}{dt}\right)^2 + \left(\frac{dz}{dt}\right)^2\right) + \left(x\,\frac{dy}{dt} - \frac{dx}{dt}\,y\right) + \frac{1}{2}(x^2+y^2) \qquad \text{(B-5)}$$

$$U = -\frac{\mu_1}{r_1} - \frac{\mu_2}{r_2} \qquad \text{(B-6)}$$

where

$$r_1 = \left((x+\mu_1)^2 + y^2 + z^2\right)^{1/2}$$
$$r_2 = \left((x-\mu_2)^2 + y^2 + z^2\right)^{1/2} \qquad \text{(B-7)}$$

By use of Lagrange's formulation, equations of motion are derived as shown below from Eq.(B-2) and Eq.(B-5) through Eq.(B-7).

$$\begin{aligned}
\frac{d^2x}{dt^2} - 2\frac{dy}{dt} - x &= -\frac{dU}{dx} \\
\frac{d^2y}{dt^2} + 2\frac{dx}{dt} - y &= -\frac{dU}{dy} \\
\frac{d^2z}{dt^2} &= -\frac{dU}{dz}
\end{aligned} \tag{B-8}$$

Introducing modified potential energy Ω, equations of motion are transformed to as follows;

$$\begin{aligned}
\frac{d^2x}{dt^2} - 2\frac{dy}{dt} &= \frac{\delta\Omega}{\delta x} \\
\frac{d^2y}{dt^2} + 2\frac{dx}{dt} &= \frac{\delta\Omega}{\delta y} \\
\frac{d^2z}{dt^2} &= \frac{\delta\Omega}{\delta z}
\end{aligned} \tag{B-9}$$

where Ω and partial derivatives $\delta\Omega/\delta x$, $\delta\Omega/\delta y$ and $\delta\Omega/\delta z$ equal to as follows;

$$\Omega = \frac{1}{2}\left(x^2 + y^2\right) + \frac{\mu_1}{r_1} + \frac{\mu_2}{r_2} + \frac{\mu_1\mu_2}{2} \tag{B-10}$$

or

$$\Omega = \frac{1}{2}\left(\mu_1 r_1^2 + \mu_2 r_2^2\right) + \frac{\mu_1}{r_1} + \frac{\mu_2}{r_2} \qquad \text{(for two-dimensional case)} \tag{B-11}$$

and

$$\begin{aligned}
\frac{\delta\Omega}{\delta x} &= x - \frac{\mu_1}{r_1^2}\left(\frac{x+\mu_2}{r_1}\right) - \frac{\mu_2}{r_2^2}\left(\frac{x-\mu_2}{r_2}\right) \\
\frac{\delta\Omega}{\delta y} &= y - \frac{\mu_1}{r_1^2}\left(\frac{y}{r_1}\right) - \frac{\mu_2}{r_2^2}\left(\frac{y}{r_2}\right) \\
\frac{\delta\Omega}{\delta z} &= -\frac{\mu_1}{r_1^2}\left(\frac{z}{r_1}\right) - \frac{\mu_2}{r_2^2}\left(\frac{z}{r_2}\right)
\end{aligned} \tag{B-12}$$

(2) Jacobi Integral (Jacobi Constant)

Energy integral of Eq.(B-9) gives the following.

$$\int\left(2\frac{dx}{dt}\frac{\delta\Omega}{\delta x}+2\frac{dy}{dt}\frac{\delta\Omega}{\delta y}+2\frac{dz}{dt}\frac{\delta\Omega}{\delta z}\right)dt=2\Omega=v^2+C \qquad \text{(B-13)}$$

where C is the integration constant and v is total velocity in rotating frame as follows:

$$v^2=\left(\frac{dx}{dt}\right)^2+\left(\frac{dy}{dt}\right)^2+\left(\frac{dz}{dt}\right)^2 \qquad \text{(B-14)}$$

These in turn give the following Eq.(B-15).

$$C=2\Omega-v^2=x^2+y^2+\frac{2\mu_1}{r_1}+\frac{2\mu_2}{r_2}+\mu_1\mu_2-v^2 \qquad \text{(B-15)}$$

This integration constant C is called Jacobi integral that stands for energy level in restricted three-body problem. Jacobi integral expressed by Eq.(B-15) has the opposite sense of energy as velocity increase brings about decrease in Jacobi integral.

(3) C3 with Respect to the Moon and Earth

Next, C_3 with respect to the primaries is highlighted. Differentiation of Eq.(B-1) yields the following.

$$\begin{pmatrix}\frac{d\xi}{dt}\\ \frac{d\eta}{dt}\\ \frac{d\zeta}{dt}\end{pmatrix}=\begin{pmatrix}+\frac{dx}{dt}\cos\psi-x\sin\psi-\frac{dy}{dt}\sin\psi-y\cos\psi\\ +\frac{dx}{dt}\sin\psi+x\cos\psi+\frac{dy}{dt}\cos\psi-y\sin\psi\\ \frac{dz}{dt}\end{pmatrix} \qquad \text{(B-16)}$$

Eq.(B-16) corresponds to S/C velocity in inertial frame, while state vectors of the earth and moon are expressed as follows (see Fig.B-1);

$$\begin{pmatrix} \xi_{moon} \\ \eta_{moon} \\ \zeta_{moon} \end{pmatrix} = \begin{pmatrix} +\mu_1 \cos\psi \\ +\mu_1 \sin\psi \\ 0 \end{pmatrix}, \quad \begin{pmatrix} d(\xi_{moon})/dt \\ d(\eta_{moon})/dt \\ d(\zeta_{moon})/dt \end{pmatrix} = \begin{pmatrix} -\mu_1 \sin\psi \\ +\mu_1 \cos\psi \\ 0 \end{pmatrix} \tag{B-17}$$

$$\begin{pmatrix} \xi_{earth} \\ \eta_{earth} \\ \zeta_{earth} \end{pmatrix} = \begin{pmatrix} -\mu_2 \cos\psi \\ -\mu_2 \sin\psi \\ 0 \end{pmatrix}, \quad \begin{pmatrix} d(\xi_{earth})/dt \\ d(\eta_{earth})/dt \\ d(\zeta_{earth})/dt \end{pmatrix} = \begin{pmatrix} +\mu_2 \sin\psi \\ -\mu_2 \cos\psi \\ 0 \end{pmatrix} \tag{B-18}$$

Then S/C's relative position and velocity w.r.t. primaries (r_M, V_M: moon, r_E,V_E: earth) in inertial frame are obtained as follows;

$$r_M^2 = (x^2+y^2+z^2) - 2\mu_1 x + \mu_1^2 \tag{B-19}$$

$$V_M^2 = \left(\left(\frac{dx}{dt}\right)^2+\left(\frac{dy}{dt}\right)^2+\left(\frac{dz}{dt}\right)^2\right)+ 2\left(x\,\frac{dy}{dt} - \frac{dx}{dt}\,y\right)+ (x^2+y^2) + 2\mu_1\left(-x - \frac{dy}{dt}\right) + \mu_1^2 \tag{B-20}$$

$$r_E^2 = (x^2+y^2+z^2) + 2\mu_2 x + \mu_2^2 \tag{B-21}$$

$$V_E^2 = \left(\left(\frac{dx}{dt}\right)^2+\left(\frac{dy}{dt}\right)^2+\left(\frac{dz}{dt}\right)^2\right)+ 2\left(x\,\frac{dy}{dt} - \frac{dx}{dt}\,y\right)+ (x^2+y^2) + 2\mu_2\left(+x + \frac{dy}{dt}\right) + \mu_2^2 \tag{B-22}$$

Finally, C3 w.r.t.moon and earth are derived from the following Eq.(B-23).

$$\text{C3.moon} = V_M^2 - \frac{2\mu_2}{r_M}$$
$$\text{C3.earth} = V_E^2 - \frac{2\mu_1}{r_E} \tag{B-23}$$

where r_M, V_M, r_E,V_E can be found in Eq.(B-19)~Eq.(B-22).

(4) Expression in Polar Coordinate

Here, lunicentric polar coordinate defined in primaries-fixed rotating frame shown below is introduced. Note that position and velocity are defined separately (see Fig.B-2).

$$\text{position} \quad \begin{aligned} x &= \mu_1 + r_M \cos\alpha_M \cos\theta_M \\ y &= r_M \cos\alpha_M \sin\theta_M \\ z &= r_M \sin\alpha_M \end{aligned} \tag{B-24}$$

$$\text{velocity} \quad \begin{aligned} dx/dt &= v_M \cos\beta_M \cos\delta_M \\ dy/dt &= v_M \cos\beta_M \sin\delta_M \\ dz/dt &= v_M \sin\beta_M \end{aligned} \tag{B-25}$$

r_M and v_M are lunicentric distance and magnitude of velocity in rotating frame, severally. Directions of S/C position and velocity are designated by (θ_M,α_M) and (δ_M,β_M), independently.

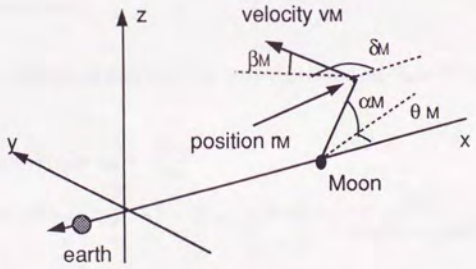

Fig.B-2 State Vector in Polar Coordinate
where Position and Velocity are Independently Defined

With this coordinate, C3 w.r.t. moon and Jacobi integral are expressed as shown below by use of Eq.(B-15) and Eq.(B-19) through Eq.(B-23).

$$C3.moon = v_M^2 + 2r_M v_M \cos\alpha_M \cos\beta_M \sin(\delta_M-\theta_M) + r_M^2 \cos^2\alpha_M - \frac{2\mu_2}{r_M} \tag{B-26}$$

$$C3.earth = v_M^2 + 2r_M v_M \cos\alpha_M \cos\beta_M \sin(\delta_M-\theta_M) + r_M^2 \cos^2\alpha_M + 1 + 2r_M\cos\alpha_M\cos\theta_M + 2v_M\cos\beta_M\sin\delta_M - \frac{2\mu_1}{(1+r_M^2+2r_M\cos\alpha_M\cos\theta_M)^{1/2}} \tag{B-27}$$

$$C = (\mu_1+ r_M\cos\alpha_M \cos\theta_M)^2 + (r_M \cos\alpha_M \sin\theta_M)^2 + \frac{2\mu_1}{(1+2r_M \cos\alpha_M \cos\theta_M + r_M^2)^{1/2}} + \frac{2\mu_2}{r_M} + \mu_1\mu_2 - v_M^2 \tag{B-28}$$

Now, some specific cases are investigated concerning C3 w.r.t. primaries at perilune. Eq.(B-26) and Eq.(B-27) are simplified to the equations below on the assumptions noted there.

(a) at perilune with planar direct motion ($\alpha_M=\beta_M=0$ and $\delta_M-\theta_M=+90$ deg)

$$C3.moon = (v_M+ r_M)^2 - \frac{2\mu_2}{r_M} \tag{B-29}$$

$$C3.earth = (v_M+ r_M)^2 + 1 + 2(r_M+v_M)\cos\theta - \frac{2\mu_1}{(1+r_M^2+2r_M\cos\theta)^{1/2}} \tag{B-30}$$

(b) at perilune with planar retrograde motion ($\alpha_M=\beta_M=0$ and $\delta_M-\theta_M= -90$ deg)

$$C3.moon = (v_M - r_M)^2 - \frac{2\mu_2}{r_M} \tag{B-31}$$

$$C3.earth = (v_M - r_M)^2 + 1 + 2(r_M - v_M)\cos\theta - \frac{2\mu_1}{(1+r_M^2+2r_M\cos\theta)^{1/2}} \tag{B-32}$$

(c) at perilune over lunar pole (α_M=90deg, β_M=0)

$$C3.moon = v_M^2 - \frac{2\mu_2}{r_M} \tag{B-33}$$

$$C3.earth = v_M^2 + 1 + 2v_M \sin\delta - \frac{2\mu_1}{(1+r_M^2)^{1/2}} \tag{B-34}$$

Note that C3 w.r.t. moon is independent of positional phase (i.e.θ_M) for planar cases (see Eq.B-29) and Eq.(B-31)), and of velocity direction (i.e.δ_M) for perilune located over lunar pole (see Eq.(B-33)).

Appendix C Cartesian Coordinate Formulation of Three-Body System (Inertial Frame)

Restricted three-body problem is formulated in inertial frame with the moon as origin by use of cartesian coordinate. Two primary bodies are assumed to be constituted of the earth and moon. The moon is assumed to orbit around the earth in circular motion. Mass of the earth and the moon is μ_1(=0.9878493317) and μ_2(=0.0121506683), severally. In Fig.C-1, (ξ,η,ζ) denotes inertial frame where earth and moon are postulated to be coincidentally located at (-μ1,0,0) and (+μ2,0,0).

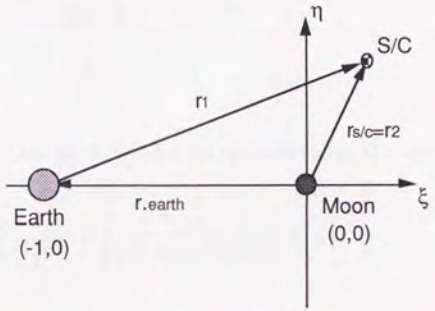

Fig.C-1 Moon-Centered Coordinate

Equations of motion are derived based on Lagrange's formulation. Kinetic energy T and effective potential energy U, which contains the effect that moon rotates around earth, are expressed as follows;

$$T = \frac{1}{2}\left(\left(\frac{d\xi}{dt}\right)^2+\left(\frac{d\eta}{dt}\right)^2+\left(\frac{d\zeta}{dt}\right)^2\right) \qquad \text{(C-1)}$$

$$U = -\frac{\mu_2}{r_2} - \mu_1\left[\frac{1}{r_1} - \frac{(r_{s/c}\cdot r_{earth})}{r_{o\text{-}earth}{}^3}\right] \qquad \text{(C-2)}$$

where r_1, r_2 and $r_{o\text{-earth}}$ are S/C-earth, S/C-moon and origin-earth (i.e.earth-moon) distance, respectively as shown below.

$$r_1 = \left((\xi+1)^2 + \eta^2 + \zeta^2\right)^{1/2}$$
$$r_2 = \left(\xi^2 + \eta^2 + \zeta^2\right)^{1/2}$$
$$r_{o\text{-earth}} = 1 \qquad \text{(C-3)}$$

$r_{s/c}$ and r_{earth} are position vectors of S/C and the earth severally as follows;

$$r_{s/c} = \begin{bmatrix} \xi \\ \eta \\ \zeta \end{bmatrix}, \quad r_{earth} = \begin{bmatrix} -1 \\ 0 \\ 0 \end{bmatrix} \qquad \text{(C-4)}$$

Using Eq.(C-3) and Eq.(C-4), effective potential energy U is rewritten as follows;

$$U = -\frac{\mu_2}{\left[\xi^2+\eta^2+\zeta^2\right]^{1/2}} - \mu_1\left[\frac{1}{\left((\xi+1)^2+\eta^2+\zeta^2\right)^{1/2}} + \xi\right] \qquad \text{(C-5)}$$

By use of Lagrange's formulation, equations of motion are derived from Eq.(C-1) and Eq.(C-5) as shown below.

$$\frac{d^2\xi}{dt^2} = -\mu_1(\xi+1)\left[(\xi+1)^2+\eta^2+\zeta^2\right]^{-3/2} - \mu_2\xi\left[(\xi^2+\eta^2+\zeta^2)^{-3/2}\right] + \mu_1$$
$$\frac{d^2\eta}{dt^2} = -\mu_1(\eta\ \ )\left[(\xi+1)^2+\eta^2+\zeta^2\right]^{-3/2} - \mu_2\eta\left[(\xi^2+\eta^2+\zeta^2)^{-3/2}\right] \qquad \text{(C-6)}$$
$$\frac{d^2\zeta}{dt^2} = -\mu_1(\zeta\ \ )\left[(\xi+1)^2+\eta^2+\zeta^2\right]^{-3/2} - \mu_2\zeta\left[(\xi^2+\eta^2+\zeta^2)^{-3/2}\right]$$

Appendix D. Cartesian Coordinate Formulation of Four-Body Problem

Formulation of restricted four-body problem is outlined where the earth and moon comprise two primaries [81]. The moon is postulated to orbit around the earth in circular motion. In addition, the sun depicts a circular orbit around the barycenter of the earth and the moon in the same plane (see Fig.D-1). In Fig.D-1, (ξ,η,ζ) and (x,y,z) denotes S/C position in inertial and primaries-fixed rotating frame, respectively. In both frames, barycenter of the earth and moon is taken as the origin. Mass of the earth and the moon is μ_1 (=0.9878493317) and μ_2 (=0.0121506683) and their positions are denoted as $(-\mu_2,0,0)$ and $(\mu_1,0,0)$, respectively in primaries-fixed rotating frame. Restricted three-body problem results simply by setting solar gravity constant as zero in this four-body formulation.

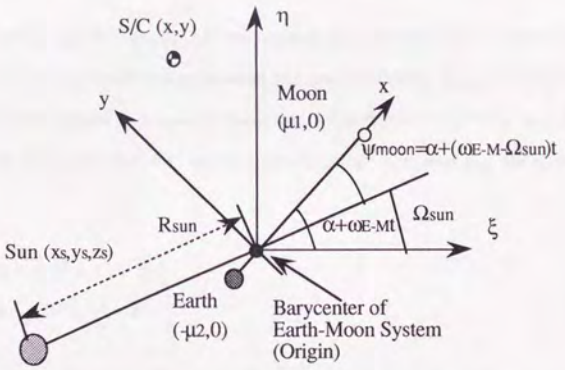

Fig.D-1 Restricted Four-Body Model (Cartesian Coordinate)

(1) Equations of Motion

Derivation of equations of motion in Lagrange's formulation is summarized below. Firstly, Lagrangian is expressed as follows;

$$L = T - U \tag{D-1}$$

where T is kinetic energy and U is potential energy as shown below. U takes the form of effective potential energy where the effect that sun rotates around the barycenter of earth-moon system (origin) is taken into account.

$$T = \frac{1}{2}\left(\left(\frac{d\xi}{dt}\right)^2+\left(\frac{d\eta}{dt}\right)^2+\left(\frac{d\zeta}{dt}\right)^2\right)$$

$$= \frac{1}{2}\left(\left(\frac{dx}{dt}\right)^2+\left(\frac{dy}{dt}\right)^2+\left(\frac{dz}{dt}\right)^2\right)+\left(x\,\frac{dy}{dt} - \frac{dx}{dt}\,y\right)+\frac{1}{2}\left(x^2+y^2\right) \tag{D-2}$$

$$U = -\frac{\mu_1}{r_1} - \frac{\mu_2}{r_2} - \mu_{sun}\left[\frac{1}{r_{sun}} - \frac{xx_s+yy_s+zz_s}{R_{sun}^3}\right] \tag{D-3}$$

where r_1 r_2 and r_{sun} are S/C-earth, S/C-moon and S/C-sun distance respectively, while R_{sun} (=389.1723985) is the distance between sun and the origin. (x_s,y_s,z_s) corresponds to sun's position with regard to origin in earth-moon fixed rotating frame. μ_{sun} is gravity constant of the sun (=328900.48) under normalization. r_1 r_2 and r_{sun} are expressed as follows;

$$r_1^2 = (x + \mu_2)^2 + y^2 + z^2 \tag{D-4}$$

$$r_2^2 = (x - \mu_1)^2 + y^2 + z^2 \tag{D-5}$$

$$r_{sun}^2 = (x - x_s)^2 + (y - y_s)^2 + (z - z_s)^2$$
$$= (x + R_{sun}\cos\psi_{moon})^2 + (y - R_{sun}\sin\psi_{moon})^2 + z^2 \tag{D-6}$$

where ψ_{moon} corresponds to moon's positional phase in sun-earth fixed rotating frame (see Fig.D-1). ψ_{moon} is described as follows;

$$\psi_{moon} = \alpha + (\omega_{E\text{-}M} - \Omega_{sun})\, t \qquad \text{(D-7)}$$

Each parameter used in Eq.(D-7) is summarized here.

α: initial sun phase angle expressed by (anti-sun direction)-(origin)-(moon) which is equivalent to initial moon's positional phase in sun-earth fixed rotating frame,

$\omega_{E\text{-}M}$: angular velocity of the earth and moon around their origin (=1.00),

Ω_{sun}: angular velocity of the sun around the origin (=0.07480133).

By use of Lagrangian formulation, equations of motion are expressed as follows;

$$\frac{d^2x}{dt^2} - 2\frac{dy}{dt} - x - \frac{\mu_{sun}}{R_{sun}^2}\cos\psi_{moon} = -\frac{\delta U_n}{\delta x}$$

$$\frac{d^2y}{dt^2} + 2\frac{dx}{dt} - y + \frac{\mu_{sun}}{R_{sun}^2}\sin\psi_{moon} = -\frac{\delta U_n}{\delta y}$$

$$\frac{d^2z}{dt^2} = -\frac{\delta U_n}{\delta z} \qquad \text{(D-8)}$$

where

$$U_n = -\frac{\mu_1}{r_1} - \frac{\mu_2}{r_2} - \frac{\mu_{sun}}{r_{sun}} \qquad \text{(D-9)}$$

and

$$\frac{\delta U_n}{\delta x} = \frac{\mu_1}{r_1^3}(x+\mu_2) + \frac{\mu_2}{r_2^3}(x-\mu_1) + \frac{\mu_{sun}}{r_3^3}(x+R_{sun}\cos\Psi_{moon})$$

$$\frac{\delta U_n}{\delta y} = \frac{\mu_1}{r_1^3}(y) + \frac{\mu_2}{r_2^3}(y) + \frac{\mu_{sun}}{r_{sun}^3}(y - R_{sun}\sin\Psi_{moon})$$

$$\frac{\delta U_n}{\delta z} = \frac{\mu_1}{r_1^3}(z) + \frac{\mu_2}{r_2^3}(z) + \frac{\mu_{sun}}{r_{sun}^3}(z) \qquad \text{(D-10)}$$

(2) S/C Positional Phase in Different Frames

Here, relation between S/C's positional phase in different frames is discussed. First, S/C positional phase in sun-earth and earth-moon fixed frame are denoted as $\theta_{S\text{-}E}$ and $\theta_{E\text{-}M}$, respectively. Remembering that Ψ_{moon} is moon's position in sun-earth fixed frame, their relation is expressed as follows (see Fig.D-2);

$$\Psi_{moon} = \theta_{S\text{-}E} - \theta_{E\text{-}M} \qquad \text{(D-11)}$$

Substitution of Eq.(D-7) for Eq.(D-11) yields Eq.(D-12) below which gives transformation of S/C position in earth-moon fixed frame ($\theta_{E\text{-}M}$) to that in sun-earth fixed frame ($\theta_{S\text{-}E}$) at an arbitrary epoch.

$$\theta_{S\text{-}E} = \theta_{E\text{-}M} + \alpha + (\omega_{E\text{-}M} - \Omega_{sun})\, t \qquad \text{(D-12)}$$

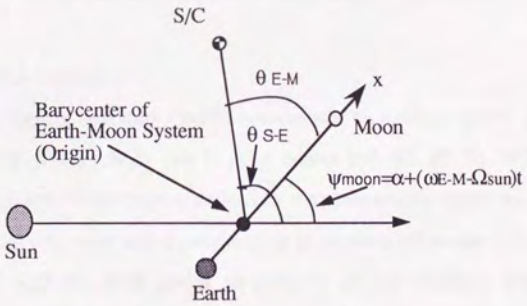

Fig.D-2 S/C Positional Phase

Appendix E Boundary between Central Attraction and Disturbing Bodies

(1) Classical Sphere of Influence

The concept of sphere of influence (SOI) was originally suggested by Laplace. SOI gives the appropriate body to which the motion of S/C is to be referred, when considering the motion of S/C in the presence of two primary bodies [92]. First, the ratio of the disturbing force to the corresponding central attraction is defined at both primaries. SOI is defined at the boundary where these two ratios are equal, and expressed numerically as shown below. Planetary sphere of influences are tabulated in Table 4-1.

$$\frac{r}{\rho} = \left(\frac{m_1}{m_3}\right)^{2/5} \qquad \text{(E-1)}$$

where m_1 and m_3 are mass of the primary body and mass of disturbing third body, respectively. r is S/C-primary body distance, while ρ is primary-third body distance.

(2) Weak Stability Boundary

Weak stability boundary (WSB) corresponds to realistic sphere of influence defined at some primary body due to other bodies [64, 69, 71-72]. WSB is a six-dimensional position-velocity space defined by the altitude with certain initial velocity, where eccentricity becomes one (corresponding to parabola) after one cycle around the primary (see Fig.E-1). WSB yields an estimate of the transition regions about gravitational mass points in the n-body problem.

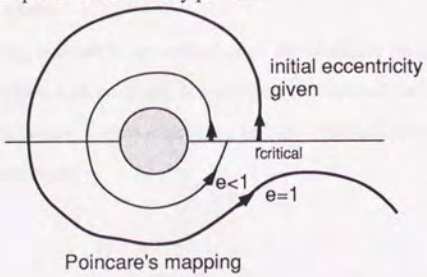

Fig.E-1 Schematic Diagram of Weak Stability Boundary

Appendix F Orbit Design Method under Two-Body Conic Approximation

(1) Patched Conic Method

Patched conic method is the most fundamental technique conventionally used in preliminary mission analysis. Suppose that S/C is moving outside the sphere of influence of primary body, the motion is ruled by the third primary body (e.g. in interplanetary trajectory, Jupiter is considered the primary body with sun as the third primary.), When it is inside the sphere of influence, S/C motion is described by two-body conic trajectory with primary body as a central attraction (usually hyperbolic trajectory). At the sphere of influence, these two-body trajectories are connected by exchanging their central body. When the radius of sphere of influence is reduced to zero, this method is called one-point patched conic method.

(2) Pseudo-State Theory

The objective of pseudo-state theory is the reduction of computing cost while retaining considerably higher precision than acquired by patched conic method [93]. Pseudo-state theory is based on the assumption that S/C conic motion around the primary and the pseudo-conic displacement due to a third body may be superimposed under some restrictions. Lambert problem (two-body problem) is solved between two pseudostates, obtained by iteration on two displacement vectors off the planetary ephemeris positions on the dates of departure and arrival.

(3) Multi-Conic Theory

Multi-conic method is an extension of pseudo-state theory [94]. Pseudo-conic displacement due to a third body is extended to multi-disturbing bodies, which is superimposed with conic motion around the primary. This results in trajectory generation by multi-conic combination.

Appendix G Fixed Time-of-Arrival Target

When positional deviation at a prescribed epoch (t_F) exists, Fixed Time-of-Arrival (FTA) guidance provides initial velocity correction at t_0 to cancel positional deviation at t_F (see Fig.G-1).

Suppose that both initial epoch (t_0) and position are given [92]. Here, transition matrix from t_0 to t_f is assumed in the following form.

$$\Phi(t_f,t_0) = \begin{pmatrix} \Phi_{11} & \Phi_{12} \\ \Phi_{21} & \Phi_{22} \end{pmatrix} \tag{G-1}$$

where Φ_{11}, Φ_{12}, Φ_{21} and Φ_{22} are 3x3 partitioned transition matrix. With Eq.(G-1), the following equations are derived.

$$\begin{pmatrix} dr(t_f)^- \\ dv(t_f)^- \end{pmatrix} = \Phi(t_f,t_0)x(t_0) = \Phi(t_f,t_0)\begin{pmatrix} dr(t_0) \\ dv(t_0) \end{pmatrix} \tag{G-2}$$

$$\begin{pmatrix} dr(t_f)^+ \\ dv(t_f)^+ \end{pmatrix} = \Phi(t_f,t_0)\begin{pmatrix} dr(t_0) \\ dv(t_0)+dV_0 \end{pmatrix} \tag{G-3}$$

where dV_0 is velocity correction at t_0 and dr and dv are position and velocity deviation, respectively. Superscript + and - each corresponds to the case with and without dV_0. Here, considering that the objective of FTA is to cancel $dr(t_f)^+$, the following equation is satisfied referring to Eq.(G-3).

$$\Phi_{11}(t_f,t_0)dr(t_0) + \Phi_{12}(t_f,t_0)(dv(t_0)+dV_0) = 0 \tag{G-4}$$

which yields,

$$\begin{aligned} \Phi_{12}dV_0 &= -\Phi_{11}(t_f,t_0)dr(t_0) - \Phi_{12}(t_f,t_0)dv(t_0) \\ &= -\left[\Phi_{11}(t_f,t_0)\ \Phi_{12}(t_f,t_0)\right]dx(t_0) \end{aligned} \tag{G-5}$$

Therefore,

$$dV_0 = - \Phi_{12}(t_f,t_0)^{-1} \left[\Phi_{11}(t_f,t_0)\ \Phi_{12}(t_f,t_0)\right] dx(t_0) \qquad \text{(G-6)}$$

From Eq.(G-2), when dV_0 is not performed at t_0, positional deviation at t_f is as follows;

$$dr(t_f)^- = \left[\Phi_{11}(t_f,t_0)\ \Phi_{12}(t_f,t_0)\right] dx(t_0) \qquad \text{(G-7)}$$

With Eq.(G-6) and Eq.(G-7), velocity correction at t_0 (i.e. dV_0) is obtained as follows;

$$dV_0 = - \Phi_{12}(t_f,t_0)^{-1}\ dr(t_f)^- \qquad \text{(G-8)}$$

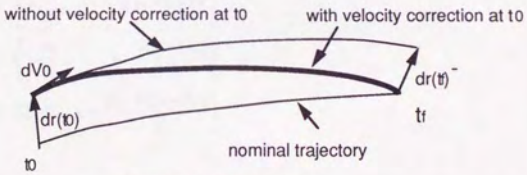

Fig.G-1 FTA Guidance

Appendix H Runge-Kutta-Merson Integration Method

Runge-Kutta-Merson method is a fifth order numerical integration method. It contains automatic step size control based on the magnitude of error. Algorithm is shown below.

Consider differential equations as follows;

$$\frac{dx}{dt} = f(x,t) \qquad \text{(t: time, x: n x 1-state vector)} \tag{H-1}$$

Then state vectors at t = t+h are calculated as follows;

$$\begin{aligned}
k_1 &= h * f[t\ ,\ x] \\
k_2 &= h * f\left[t+\frac{h}{3}\ ,\ x+\frac{k_1}{3}\right] \\
k_3 &= h * f\left[t+\frac{h}{3}\ ,\ x+\frac{k_1+k_2}{6}\right] \\
k_4 &= h * f\left[t+\frac{h}{2}\ ,\ x+\frac{k_1+3k_3}{8}\right] \\
k_5 &= h * f\left[t+h\ ,\ x+\frac{k_1-3k_3+4k_4}{2}\right]
\end{aligned} \tag{H-2}$$

$$x = x + \frac{k_1+4k_4+k_5}{6} \tag{H-3}$$

$$E = \frac{k_1 - 4.5k_3+4k_4 - 0.5k_5}{15} \tag{H-4}$$

where k_1, k_2, k_3, k_4, k_5 and E are n x 1-vectors. E corresponds to magnitude of error.

Appendix I Numerical Example of Swingby Trajectory

In Fig.I-1, an example of swingby trajectory is depicted in inertial and earth-moon fixed frame. Also local variation of C3 w.r.t. earth as well C3 w.r.t. moon are shown. In earth-moon fixed frame, trajectory goes mainly through 2nd and 1st quadrant whose orbital profile is quite different from that of gravitational capture trajectory (see Fig.3-24). Note that C3 w.r.t. earth (semi-major axis) is almost constant outside the sphere of influence, which validates the use of patched conic approximation for swingby trajectory.

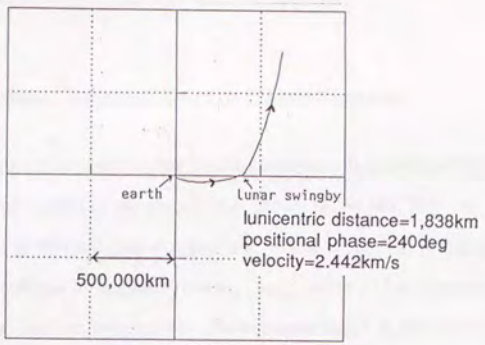

inertial frame

(swingby distance=1,838km, θ=240deg, perilune velocity=2.442km/s)

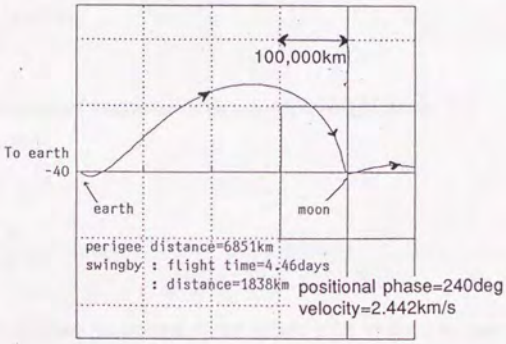

earth-moon fixed rotating frame

(perigee distance=6,851km, swingby: flight time=4.46days)

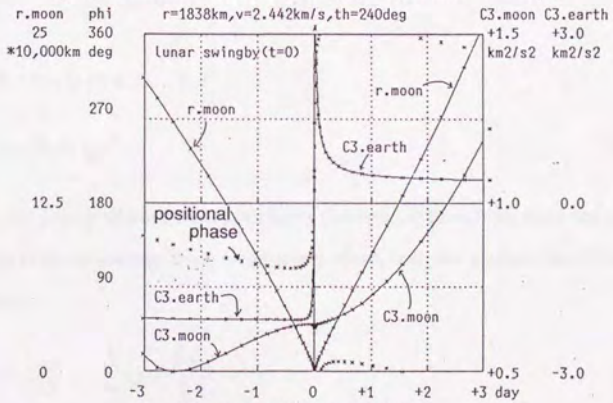

history of orbital parameters

Fig.I-1 Example of Swingby Trajectory (earth-moon-S/C three-body system)

Appendix J Multi-Swingby Trajectory Design by B-Plane Parameters

In trajectory design accompanying multi-swingbys, B-plane parameters are occasionally utilized. The outline of the algorithm is shown below [89, 90].

First, trajectory is divided into n segments, where ith epoch is defined as t_i. Velocity at the same epoch t_i in ith segment (from t_{i-1} to t_i) and in (i+1)th segment (from t_i to t_{i+1}) are nominated v_i^- and v_i^+, respectively. Performance index is defined as the sum of delta-Vs at respective joint point as follows;

$$F = \sum_{i=0}^{n-1} f_i \Delta v_i^T \Delta v_i \tag{J-1}$$

where Δv_i is the required maneuver delta-V and f_i is weight factor.

$$\Delta v_i = v_i^+ - v_i^- \tag{J-2}$$

$$f_i = \frac{1}{|\Delta v_i|} \tag{J-3}$$

To minimize F, B-plane parameters p_i and epochs t_i are updated as control parameters. Here, swingby of n times is considered where independent variables are defined as follows;

$$X = (p_1\ t_1\ p_2\ t_2\ \ldots\ldots\ p_n)^T \tag{J-4}$$

$$p_i = (h_i\ \theta_i\ t_{pi})^T \tag{J-5}$$

where $h_i\ \theta_i\ t_{pi}$ are perilune distance (swingby distance), approaching angle defined at B-plane and perilune passage time, respectively. Here, both the gradient and Hessian are considered.

$$g^T = \frac{dF}{dX} = 2\sum_{i=0}^{n} f_i \Delta v_i^T \frac{\partial \Delta v_i}{\partial X} \tag{J-6}$$

$$H = \frac{d^2E}{dX^2}$$
$$= 2 \sum_{i=0}^{n} f_i \left(\Delta v_i^T \frac{\partial^2 \Delta v_i}{\partial X^2} + \frac{\partial \Delta v_i^T}{\partial X} \frac{\partial \Delta v_i}{\partial X} \right) \quad \text{(J-7)}$$

which yields the following equation when postulating that $\frac{\partial^2 \Delta v_i}{\partial X^2}$ can be ignored when compared with $\frac{\partial \Delta v_i}{\partial X}$.

$$H = 2 \sum_{i=0}^{n} f_i \frac{\partial \Delta v_i^T}{\partial X} \frac{\partial \Delta v_i}{\partial X} \quad \text{(J-8)}$$

Next, performance index F and its derivative g are expanded in Taylor series.

$$F = F_0 + g_0^T(X-X_0) + \frac{1}{2}(X-X_0)^T H_0(X-X_0) + \ldots \quad \text{(J-9)}$$

$$g = g_0 + H_0(X-X_0) + \ldots \quad \text{(J-10)}$$

Provided that local minimum of performance index F exists, control parameter X which minimize F is obtained in the following manner.

$$g = \frac{\partial F}{\partial X} = 0 \quad \text{(J-11)}$$

which yields

$$X = X_0 - H_0^{-1} g_0 \quad \text{(J-12)}$$

The partial derivatives of the velocity discontinuities with respect to the independent variables $\frac{\partial \Delta v_i}{\partial X}$ are found as follows which are used in the computation of gradient vector and Hessian matrix of performance index F;

$$\frac{\partial \Delta v_i}{\partial p_j} = \begin{cases} O & (0 \le i \le j-2) \\ U_j & (i=j-1) \\ (W_{j+1}B_j - D_j)U_j & (i=j) \\ (W_{j+2}ABW_{j+1} - CDW_{j+1})B_jU_j & (i=j+1) \\ (W_{i+1}ABW_i - CDW_i)(\prod_{k=j+1}^{i-1} ABW_k)B_jU_j & (j+2 \le i \le n-1) \end{cases} \quad \text{(J-13)}$$

$$\frac{\partial \Delta v_i}{\partial t_j} = \begin{cases} O & (0 \le i \le j-1) \\ - W_{j+1}\Delta v_j & (i=j) \\ - (W_{j+2}ABW_{j+1} - CDW_{j+1})\Delta v_j & (i=j+1) \\ - (W_{i+1}ABW_i - CDW_i)(\prod_{k=j+1}^{i-1} ABW_k)\Delta v_j & (j+2 \le i \le n-1) \end{cases} \quad \text{(J-14)}$$

where

$$ABW_i = A_i + B_iW_i \quad \text{(J-15)}$$

$$CDW_i = C_i + D_iW_i \quad \text{(J-16)}$$

$$\Phi(t_i, t_{i-1}) = \begin{bmatrix} A_i & B_i \\ C_i & D_i \end{bmatrix} \quad \text{(J-17)}$$

$\Phi(t_i, t_{i-1})$ is state transition matrix of the ith trajectory segment.

$$W_i = \frac{\partial v_{i-1}^+}{\partial R_{i-1}} \Big| t_{i-1}, p_i \quad \text{(J-18)}$$

$$U_i = \frac{\partial v_{i-1}^+}{\partial p_i} \Big| t_{i-1}, R_{i-1} \quad \text{(J-19)}$$

where R_{i-1} is initial position at ith trajectory segment. W_i gives the effect of initial position of the ith trajectory segment on initial velocity when targeting from a fixed initial time to fixed B-plane parameters, while U_i gives the variation of the initial velocity on the ith trajectory segment with respect to B-plane parameters when targeting from a fixed time and position.

List of Figures

List of Tables

List of Symbols

Symbols which have already appeared in previous chapters are not listed.

Chapter 3

a	semi-major axis
μ	gravity constant
μ_1	gravity constant of the larger primary ($\mu_1>\mu_2$, $\mu_1+\mu_2=1$)
μ_2	gravity constant of the smaller primary ($\mu_1>\mu_2$, $\mu_1+\mu_2=1$)
ξ	cartesian coordinate in inertial frame, (ξ,η,ζ)
η	cartesian coordinate in inertial frame, (ξ,η,ζ)
ζ	cartesian coordinate in inertial frame, (ξ,η,ζ)
x	cartesian coordinate in primaries-fixed rotating frame, (x,y,z)
y	cartesian coordinate in primaries-fixed rotating frame, (x,y,z)
z	cartesian coordinate in primaries-fixed rotating frame, (x,y,z)
r	polar coordinate in primaries-fixed rotating frame (r,φ,χ) with the smaller primary as origin, S/C-primary body distance
φ	polar coordinate in primaries-fixed rotating frame (r,φ,χ) with the smaller primary as origin, S/C positional phase
χ	polar coordinate in primaries-fixed rotating frame (r,φ,χ) with the smaller primary as origin, S/C elevation angle
ψ	angle between ξ-axis of inertial and x-axis of primaries fixed rotating frame
θ_{xy}	in-plane entry position
θ_z	out-of-plane entry position
C	Jacobi integral ($C=2\Omega-v^2$)
Ω	modified potential energy in three-body system
$L_k(k=1,5)$	Lagrange points
C3	two-body energy level in osculating state
C3.moon	C_3 with respect to the moon
C3.earth	C_3 with respect to the earth
v	total velocity in primaries-fixed rotating frame
V	total velocity in inertial frame
V_{inf}	velocity at infinity

Chapter 4

r	S/C-smaller primary body distance
r_{cr}	critical distance (defined in Appendix A)
r_{L1}	smaller primary-L1 distance
r_{SOI}	radius of sphere of influence

Chapter 6

h	angular momentum

h.earth	angular momentum around the earth
e	eccentricity
p	semi-latus rectum
t_{total}	total flight time

Chapter 7

$V_{perigee}$	perigee velocity at earth departure
$\theta_{perigee}$	perigee position at earth departure
$V_{perilune}$	perilune velocity at lunar insertion
$\theta_{perilune}$	perilune position at lunar insertion
t_{total}	total flight time
α	sun phase defined at a certain epoch (e.g. moon's position in sun-earth fixed rotating frame at lunar insertion)
t_1	epochs at the end of intermediate trajectory segment
t_2	epochs at the end of intermediate trajectory segment
ΔV_1	velocity correction at terminal points of FTA guidance
ΔV_2	velocity correction at terminal points of FTA guidance
Δr_{apo}	Apogee distance deviation
$\Delta\theta_{apo}$	Apogee positional phase deviation
Δr_{swb}	Swingby distance deviation
$f_k(k=1,5)$	weight factors
X	control parameter vector
F	performance index
g	derivative of performance index F w.r.t. control parameter vector X
H	second derivative of performance index F w.r.t. control parameter vector X
γ	coefficient for updating control parameter vector
r_1	radius of initial circular orbit for circular-to-circular transfer
r_2	radius of final circular orbit for circular-to-circular transfer
r_i	apogee distance in bi-elliptic transfer

Appendix A

L	Lagrangian (L=T-U)
r_1	distance between S/C and larger primary
r_2	distance between S/C and smaller primary
T	kinetic energy
U	potential energy
ξ_{moon}	cartesian coordinate of the moon in inertial frame, $(\xi_{moon},\eta_{moon},\zeta_{moon})$
η_{moon}	cartesian coordinate of the moon in inertial frame, $(\xi_{moon},\eta_{moon},\zeta_{moon})$

ζ_{moon}	cartesian coordinate of the moon in inertial frame, (ξ_{moon},η_{moon},ζ_{moon})
ξ_{earth}	cartesian coordinate of the moon in inertial frame, (ξ_{earth},η_{earth},ζ_{earth})
η_{earth}	cartesian coordinate of the moon in inertial frame, (ξ_{earth},η_{earth},ζ_{earth})
ζ_{earth}	cartesian coordinate of the moon in inertial frame, (ξ_{earth},η_{earth},ζ_{earth})
r_E	S/C-earth distance
r_M	S/C-moon distance
V_E	S/C relative velocity w.r.t. the earth in inertial frame
V_M	S/C relative velocity w.r.t. the moon in inertial frame

Appendix B

v_M	S/C velocity in primaries-fixed rotating frame
θ_M	in-plane S/C positional phase in primaries-fixed rotating frame
α_M	out-of-plane S/C positional phase in primaries-fixed rotating frame
δ_M	in-plane S/C velocity direction in primaries-fixed rotating frame
β_M	out-of-plane S/C velocity direction in primaries-fixed rotating frame

Appendix C

$r_{S/C}$	S/C position in inertial frame with moon as origin
r_{earth}	earth's position in inertial frame with moon as origin
r_{moon}	moon's position in inertial frame with moon as origin
$r_{o\text{-}earth}$	distance between origin and the earth

Appendix D

r_{sun}	S/C-sun distance
R_{sun}	distance between the sun and barycenter of earth-moon system
μ_{sun}	gravity constant of the sun (=328900.48) under normalization
ψ_{moon}	moon's positional phase in sun-earth fixed rotating frame
α	initial sun phase angle expressed by (anti-sun direction)-(origin)-(moon) which is equivalent to initial moon's positional phase in sun-earth fixed rotating frame
$\omega_{E\text{-}M}$	angular velocity of the earth and moon around their origin (=1.00)
Ω_{sun}	angular velocity of the sun around the origin (=0.07480133)
U_n	quasi-potential energy
$\theta_{S\text{-}E}$	S/C positional phase in sun-earth fixed frame
$\theta_{E\text{-}M}$	S/C positional phase in earth-moon fixed frame

Appendix E

m_1	mass of the primary body

m_3	mass of disturbing third body
r	S/C-primary body distance
ρ	primary-third body distance

Appendix G

t_0	initial epoch
t_f	prescribed final epoch
$\Phi(t_f,t_0)$	transition matrix
$\Phi_{ij}(i,j=1,2)$	3x3 partitioned transition matrix
dV_0	velocity correction at t_0
dr	position deviation
dv	velocity deviation
+	superscript: with dV_0
-	superscript: without dV_0

Appendix H

$k_k(k=1,5)$	coefficient for Runge-Kutta-Merson method
E	magnitude of error.

Appendix J

v_i^-	velocity at the epoch t_i in ith segment (from t_{i-1} to t_i)
v_i^+	velocity at the epoch t_i in (i+1)th segment (from t_i to t_{i+1})
Δv_i	required maneuver delta-V
f_i	weight factor
p_i	B-plane parameters
h_i	perilune distance (swingby distance)
θ_i	approaching angle defined at B-plane
t_{pi}	perilune passage time
$\Phi(t_i,t_{i-1})$	state transition matrix of the ith trajectory segment
ABW_i	$A_i + B_iW_i$
CDW_i	$C_i + D_iW_i$
A_i	partitioned transition matrix of $\Phi(t_i,t_{i-1})$
B_i	partitioned transition matrix of $\Phi(t_i,t_{i-1})$
C_i	partitioned transition matrix of $\Phi(t_i,t_{i-1})$
D_i	partitioned transition matrix of $\Phi(t_i,t_{i-1})$
R_{i-1}	initial position at ith trajectory segment
W_i	the effect of initial position of the ith trajectory segment on initial velocity when targeting from a fixed initial time to fixed B-plane parameters
U_i	the variation of the initial velocity on the ith trajectory segment with respect to B-plane parameters when targeting from a fixed time and position

Acknowledgment

The author wishes to express his gratitude to Prof.H.Matsuo, chief supervisor of this thesis, of the University of Tokyo and the Institute of Space and Astronautical Science (ISAS) for the helpful and enlightening guidance. He also would like to acknowledge sincere advices of Prof.J.Kawaguchi and Dr.N.Ishii of ISAS through many discussions. Prof.K.Uesugi of ISAS gave him the opportunity to turn his eye on the unique trajectory studied in this dissertation.

Thanks are also due to Prof.M.Nagatomo, ISAS, Prof.T.Tanabe, Prof.K.Kato, the University of Tokyo and Prof.K.Kawachi, Research Center for Advanced Science and Technology, University of Tokyo, for critical reading of the manuscript and discussions.

The author is indebted to Dr.E.Belbruno of Jet Propulsion Laboratory, California Institute of Technology for helpful comments through private communication. And he appreciates the invaluable discussion with technical staffs of Mission Design Section of Jet Propulsion Laboratory when he was a one-day visitor, with special thanks to Mr.J.Miller, Dr.R.Cook and Dr.T.Sweetser.

This research was partially supported by Fellowships of the Japan Society for the Promotion of Science (JSPS) for Japanese Junior Scientists.

Finally, the author is pleased to show his gratitude to his wife Tomoko for her wholehearted support.

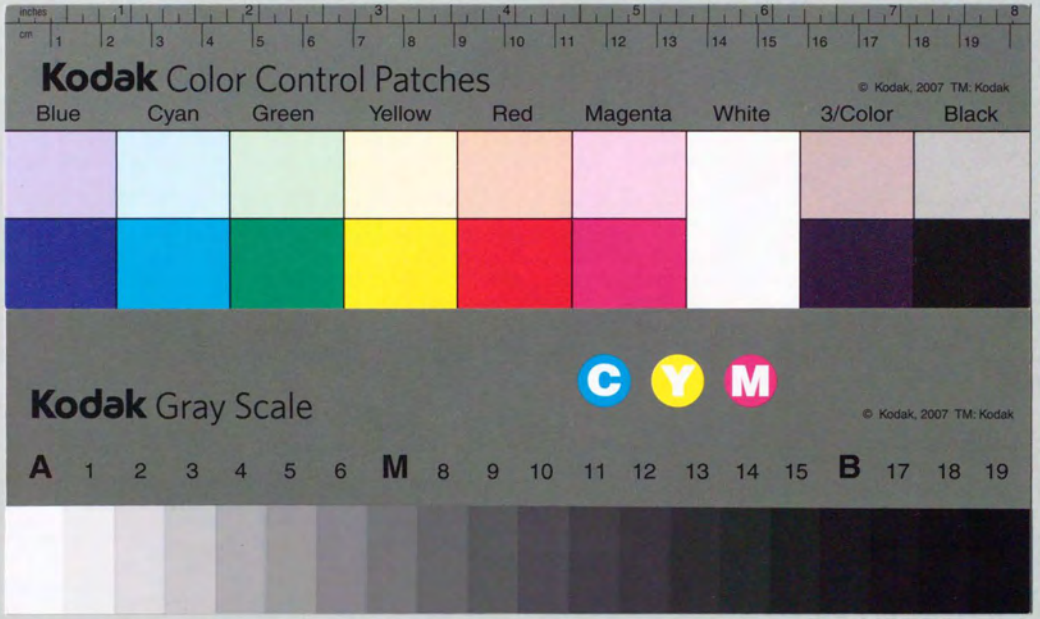
inches
cm
Kodak Color Control Patches
© Kodak, 2007 TM: Kodak
Blue
Cyan
Green
Yellow
Red
Magenta
White
3/Color
Black
Kodak Gray Scale
C
Y
M
© Kodak, 2007 TM: Kodak
A 1 2 3 4 5 6 M 8 9 10 11 12 13 14 15 B 17 18 19